

Technische Universität München  
Physik Department  
Lehrstuhl für Biophysik E22

# **Engineering of Bulk and Nanostructured GaAs with Organic Monomolecular Films**

Klaus Adlkofer

Vollständiger Abdruck der von der Fakultät für Physik der Technischen Universität  
München zur Erlangung des akademischen Grades eines Doktors der  
Naturwissenschaften genehmigten Dissertation.

Vorsitzender: Univ.-Prof. Dr. M. Kleber

Prüfer der Dissertation:

1. Univ.-Prof. Dr. E. Sackmann
2. Hon.-Prof. Dr. P. Fromherz

Die Dissertation wurde am 01.12.2003 bei der Technischen Universität München  
eingereicht und durch die Fakultät für Physik am 16.12.2003 angenommen.



## Danke!

**Prof. Erich Sackmann** für die Möglichkeit an seinem Lehrstuhl zu promovieren.

**Dr. Motomu Tanaka** für seine hervorragende Betreuung und vieles mehr.

Motomus Gruppe und den Insassen des neuen und alten Diplomandenzimmers **Oliver Purrucker, Florian Rehfeldt, Murat Tutus, Joachim Hermann, Michael Nikolaides**, und **Stephan Rauschenbach** für eine interessante und ereignisreiche Zeit.

Ein paar Ex-E22ern, **Dr. Heiko Hillebrandt, Dr. Matthias F. Schneider** und **Dr. Gerald Wiegand** für die verschiedenste Unterstützung bei dieser Arbeit.

Allen übrigen **E22ern** und **Ehemaligen** für die einzigartige Atmosphäre und Hilfe in jeder Situation.

**Prof. Gerhard Abstreiter** (Walter Schottky Institut, TU München) für die Diskussionen und Zusammenarbeit im Bereich der Nanostrukturen.

**Dr. Marc Tornow** (Walter Schottky Institut, TU München), **Sebastian Luber** und **Uli Rant** für die gute und fruchtbare Zusammenarbeit im Bereich der 2DEGs.

**Prof. M. Grunze** (Univ. Heidelberg) und seiner Gruppe für viele wichtige Elemente dieser Arbeit.

**Dr. Wolfgang Eck** für das Bereitstellen der 4-Mercaptobiphenyle.

**Dr. Michael Zharnikov** und **Dr. Andrey Shaporenko** für die große Hilfe bei den NEXAFS und HRXPS Messungen.

**Prof. Armin Gölzhäuser** (Univ. Bielefeld) und **Anne Paul** für das e-beam crosslinken der 4'-Substituierten-4-mercaptobiphenyle.

**Prof. Abraham Ulman** (Polytechnic Univ. Brooklyn, NY, USA) für fruchtbare Diskussionen und die 4'-Substituierten-4-mercaptobiphenyle.

Meinen **Eltern** für die langjährige Unterstützung.

**Karin Bucher**, die immer für mich da war.



## Table of Contents

<b>1</b>	<b>SUMMARY .....</b>	<b>1</b>
<b>2</b>	<b>INTRODUCTION .....</b>	<b>3</b>
<b>3</b>	<b>MATERIALS, PREPARATION AND METHODS.....</b>	<b>7</b>
3.1	MATERIALS .....	7
3.2	PREPARATION .....	9
3.3	MEASUREMENT METHODS.....	11
3.3.1	<i>Atomic Force Microscopy</i> .....	11
3.3.2	<i>Ellipsometry</i> .....	13
3.3.3	<i>Spectroscopic Techniques</i> .....	15
3.3.3.1	Near Edge X-Ray Fine Structure Spectroscopy .....	15
3.3.3.2	High Resolution X-Ray Photoelectron Spectroscopy.....	16
3.3.4	<i>Contact Angle Measurement</i> .....	18
3.3.5	<i>Electrochemical Measurements</i> .....	19
3.3.5.1	Cyclic Voltammetry.....	20
3.3.5.2	Impedance Spectroscopy .....	21
<b>4</b>	<b>OPTIMIZATION OF GRAFTING CONDITIONS.....</b>	<b>25</b>
4.1	IMPACT OF SOLVENTS .....	25
4.2	IMPACT OF TEMPERATURE.....	27
<b>5</b>	<b>STRUCTURAL ANALYSIS IN DRY STATES.....</b>	<b>28</b>
5.1	SURFACE TOPOGRAPHY.....	28
5.2	FILM THICKNESS.....	30
5.3	MOLECULAR ORIENTATION AND CHEMICAL COMPOSITION .....	31
5.3.1	<i>Molecular Orientation</i> .....	31
5.3.2	<i>Chemical Composition</i> .....	36
<b>6</b>	<b>STABILITY AND PROPERTIES IN ELECTROLYTE .....</b>	<b>40</b>
6.1	WETTING AND SURFACE FREE ENERGY.....	40
6.2	ELECTROCHEMICAL PROCESSES ACROSS THE INTERFACE .....	43
6.3	STABILITY AND INTERFACE PROPERTIES .....	45

<b>7</b>	<b>FUNCTIONALIZED GAAS-BASED 2DEG DEVICE .....</b>	<b>49</b>
7.1	SYSTEM AND DEVICE.....	49
7.1.1	<i>The Two-Dimensional Electron Gas System</i> .....	49
7.1.2	<i>Device</i> .....	50
7.2	DIPOLE MOMENT OF GRAFTED MOLECULES .....	52
7.3	STABILITY AND SENSITIVITY AGAINST POLAR SOLVENTS .....	56
7.4	STABILITY IN AQUEOUS ELECTROLYTE .....	59
<b>8</b>	<b>CONCLUSIONS .....</b>	<b>60</b>
	<b>LITERATURE .....</b>	<b>62</b>
	<b>PUBLICATIONS .....</b>	<b>73</b>

## 1 Summary

This thesis deals with a new method to engineer stoichiometric gallium arsenide (GaAs) [100] surfaces by deposition of organic monomolecular films, which can be used as stable and functional platforms for the design of novel bio-inspired semiconductor devices. Here, instead of commonly used inorganic insulators, a new class of self-assembled monolayers (SAMs) composed of 4-mercaptobiphenyl derivatives (X-MBPs) is used to stabilize the GaAs/electrolyte interface as well as to functionalize the GaAs surface. These functional organic “domino-like” molecules with rigid and bulky biphenyl backbones are chosen to accomplish high surface stabilities against the degradation in air and in water, and to provide various chemical functions to the surface via flexible 4'-substitutions.

In *Chapter 4*, two dominant parameters, solvent polarity and temperature, which determine the film qualities were systematically changed to optimize the grafting conditions of the X-MBPs. Qualities of the SAMs were evaluated in terms of the thickness using ellipsometry and the electrochemical stability checked by impedance spectroscopy.

In *Chapter 5*, the optimized SAMs and the bare GaAs (prepared by wet chemical etching) were characterized using various surface sensitive techniques in dry states, i.e. either in ambient or in vacuum. Atomic force microscopy (AFM) implied that the surfaces of SAMs have the comparable smoothness to bare GaAs, while ellipsometry measurements verified the monolayer formation. Near edge x-ray adsorption fine structure (NEXAFS) spectroscopy yielded the tilt angle of highly ordered MBP backbones to the surface normal. Furthermore, high resolution x-ray photoelectron spectroscopy (HRXPS) confirmed the covalent binding of sulfur and arsenide, and demonstrated the high chemical stability of the engineered surface against the oxidation in ambient.

In *Chapter 6*, the functionalized GaAs surfaces were characterized in contact with water. Firstly, the surface free energies were calculated from the contact angles of different liquid droplets, which provide quantitative measures for the surface compatibilities to lipid membranes and biopolymers. In the next step, the

electrochemical characterizations of the functionalized GaAs in physiological electrolytes were carried out by cyclic voltammetry and AC impedance spectroscopy. Cyclic voltammetry demonstrated that the grafting of SAMs resulted in a significant reduction of charge transfer across the GaAs/electrolyte interface. Furthermore, impedance spectroscopy experiments denoted excellent electrochemical stabilities of the monolayer-coated GaAs in physiological electrolytes for more than 20 h.

*Chapter 7* introduces the direct application of the established engineering protocol on the planar FET with a Hall-bar configuration, where the two-dimensional electron gas (2DEG) is confined in the vicinity of the GaAs surface. Here, the molecular dipoles from 4'-substituents and the solvent polarities were found to influence the sheet resistance of the 2DEG significantly, suggesting that the functionalized FETs are highly sensitive to the surface dipole moments.

The surface engineering method developed in the present study demonstrated a reliable device stability for the operations of various GaAs-based semiconductors with well defined surface characteristics, and suggests its large potentials to fabricate new biofunctional devices by deposition of biopolymers and model cell membranes.

## 2 Introduction

Since almost 30 years ago, there have been numerous applications of semiconductor devices as chemical sensors, where the changes on the device surface can be detected as electrical and/or optical readouts (Bergveld '03; Schöning '01; Seker et al. '00). For example, using field-effect-transistors (FETs), the changes in the surface potentials (and the resulting accumulation and depletion of charge carriers) can be detected electrically as the changes in conductance or related electrical properties. Recently, the engineering of semiconductor surfaces with bio-functional molecules has been drawing increasing attentions towards the design of a new class of biosensors (Bergveld '96; Cui et al. '01; Sackmann & Tanaka '00; Vilan et al. '03).

On the other hand, the application of semiconductor devices for biological sensors has suffered from the undesired properties of each material. For example, gallium arsenide (GaAs) has demonstrated its large potential to fabricate surface sensitive, low-dimensional structures via flexible band-gap engineerings using molecular beam epitaxy (MBE). However, the sensor operations of GaAs-based devices under physiological environments are often found to be difficult because of complex electrochemical processes at the GaAs/electrolyte interface that result in electrochemical degradation and release of poisonous arsenides. In fact, most of the electrochemical studies on GaAs have been performed under acidic or basic conditions, at which the GaAs surface is stable (Hens & Gomes '99; Miller & Richmond '97; Uhlendorf et al. '95). As generally known, the deposition of relatively thick inorganic insulators (like  $\text{SiO}_2$  and  $\text{Al}_2\text{O}_3$  (Kakimura & Sakai '79) with thickness of 50 – 100 nm) certainly improves the stability however, the large separation between the surface and the sensing layer would cause the loss of sensitivity.

One of the promising strategies to overcome such fundamental drawbacks without losing the surface sensitivity is the covalent coupling of organic monomolecular films with a typical thickness of 1 – 2 nm, such as self-assembled monolayers (SAMs) (Ulman '91; '96). Many studies have been conducted to passivate GaAs surfaces by coupling of various sulfides and mercapto compounds, but the passivation effects are

mostly discussed in dry state, i.e. either in contact with air or with metals (Asai et al. '93; Lunt et al. '91) (Miller & Richmond '97; Nakagawa et al. '91; Sheen et al. '92). However, systematic investigations on the electrochemical passivation of GaAs with SAMs in physiological electrolytes are still missing.

In 2000, we firstly accomplished the electrochemical passivation of GaAs surfaces under physiological conditions by deposition of octadecylthiol (ODT) monolayers (Adlkofer & Tanaka '01; Adlkofer et al. '00). Nevertheless, this strategy includes two fundamental drawbacks: (1) the surface pre-treatment (photochemical etching under UV irradiation) might roughen or damage the surface, and (2) gauche defects of the alkyl chains results in inhomogeneous films.

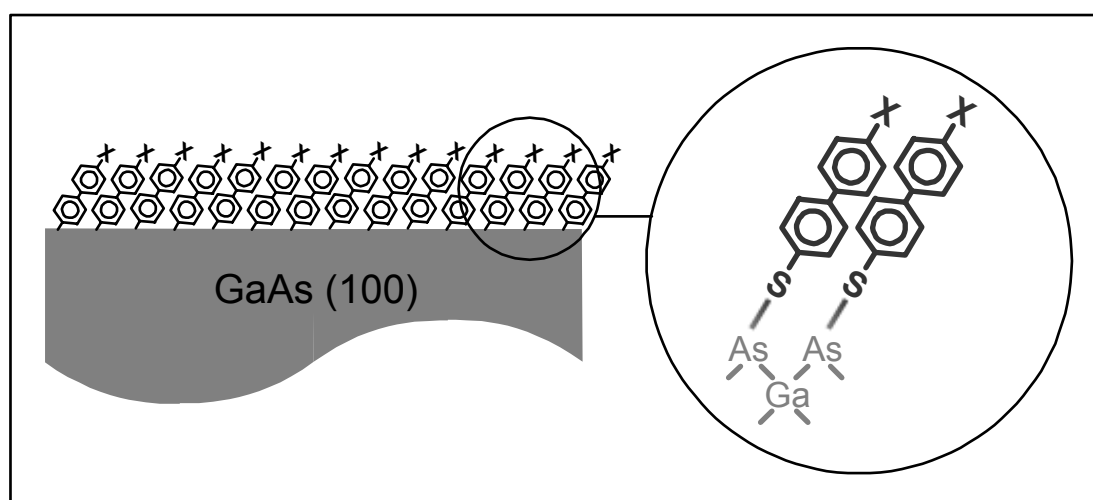


**Figure 2.1**

*Sketch of well-ordered self-assembled monolayer (SAM) of 4'-substituted-4-mercaptobiphenyl (X-MBP) on stoichiometric GaAs [100] surface.*

To solve the above mentioned problems, a new method to functionalize stoichiometric GaAs surfaces with 4-mercaptobiphenyl derivatives has been developed in the present study (Fig. 2.1). Here, 4'-substituted-4-mercaptobiphenyls (X-MBPs) with more rigid and bulkier biphenyl backbones were chosen to avoid the gauche rotation of backbones as well as to achieve high passivation efficiencies on stoichiometric GaAs [100] surfaces. Furthermore, flexible 4'-substitutions allow for the control of functionalities of the engineered surface (Kang et al. '98; Kang et al.

'99; Kang et al. '01; Ulman '01), which can provide the useful platform to design plasma membrane models by deposition of lipid membranes with membrane-associated proteins. Indeed, the wetting interactions of the engineered surface with lipid membranes are very crucial to accomplish mechanically stable composite membranes (Sackmann & Tanaka '00).

As the first step, the grafting conditions of the X-MBPs on GaAs surfaces have to be optimized. In *Chapter 4*, the impacts of solvents and reaction temperature on the layer quality have systematically been studied in terms of the film thickness and electrochemical resistivity to gain the optimal grafting conditions. After optimizing the preparation protocol, the surface topography, film thickness, backbone orientation, and chemical composition of the SAMs have been studied using various surface sensitive techniques in dry states, i.e. either in ambient or in vacuum (*Chapter 5*).

*Chapter 6* is mainly dedicated for the characterizations of GaAs surfaces coated with the X-MBP monolayers in contact with water. As the first step, the wetting conditions of the functionalized surfaces were quantitatively evaluated in terms of the surface free energies by contact angle measurements. This was followed by the electrochemical characterizations of the functionalized GaAs in physiological electrolytes. Current-voltage scans demonstrated a remarkable suppression of oxidation and reduction at the GaAs/electrolyte interface by the monolayer deposition. Furthermore, the GaAs coated with three different X-MBPs showed excellent electrochemical stabilities in the wide frequency region for more than 20 h, confirmed by AC impedance spectroscopy.

After the systematic studies of the X-MBP monolayers on bulk GaAs in air and under physiological conditions, the established engineering protocol was also transferred to the AlGaAs/GaAs heterostructures, where the two-dimensional electron gas (2DEG) is confined in the vicinity of the GaAs surface (*Chapter 7*). As depicted in *Figure 2.2*, the planar FET with a Hall-bar configuration was used to study the influence of surface dipole moments on the sheet resistance of the 2DEG (Luber et al. in print; Luber et al. '02). The electrochemical stability achieved by the optimal surface chemistry suggests a promising feature for the application of such surface-near low-dimensional semiconductors as biosensor platforms.

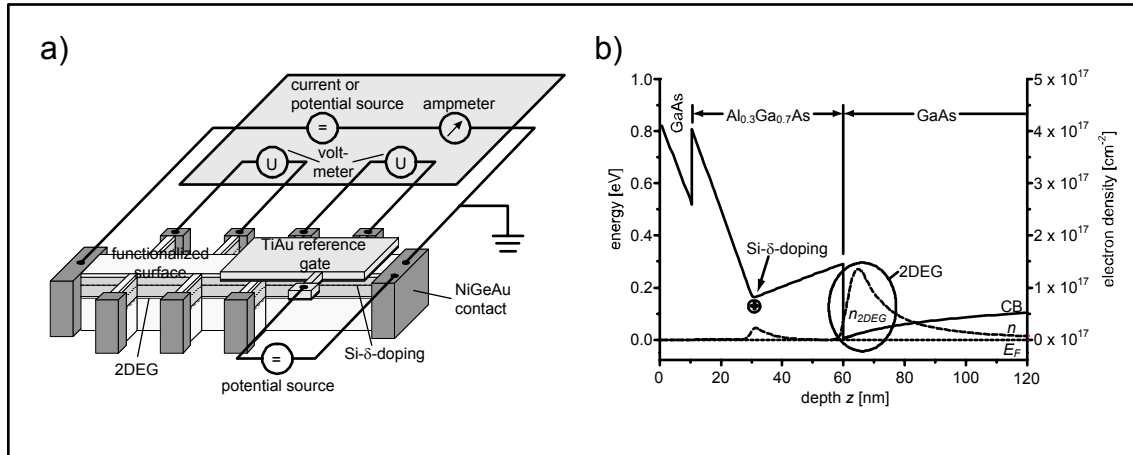


**Figure 2.2**

- a) Schematic view of the standard measurement setup for resistance measurements on the Hall-bar.
- b) Calculated (nextnano<sup>3</sup>, Walter Schottky Institute, TU München) conduction band edge (CB, solid line) and electron density ( $n$ , broken line) of the 2DEG system near the surface ( $d = 60$  nm) at 295 K.

Details of the obtained results are discussed in the following *Chapters*.

## 3 Materials, Preparation and Methods

First, the used materials and the preparation of the self-assembled monolayers (SAMs) of 4'-substituted-4-mercaptobiphenyl (X-MBP) are described. In the second part an overview of the various measure methods to analyze the gallium arsenide (GaAs) surface after the etching and grafting of the SAMs is given.

### 3.1 Materials

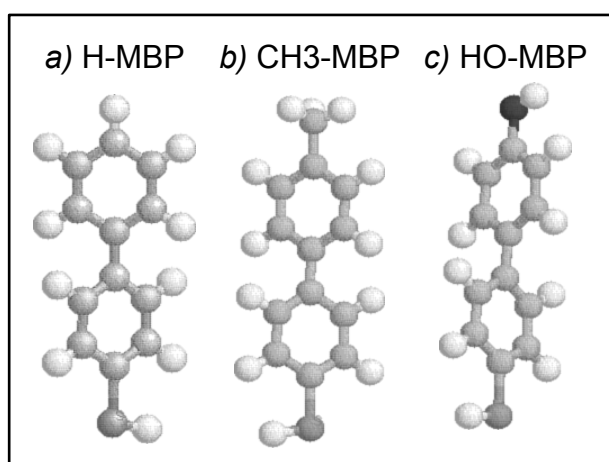


**Figure 3.1**

*Ball and stick model of*

- a) 4-mercaptobiphenyl ( $H-(C_6H_4)_2-SH$ ; H-MBP),*
- b) 4'-methyl-4-mercaptobiphenyl ( $CH_3-(C_6H_4)_2-SH$ ; CH<sub>3</sub>-MBP) and*
- c) 4'-hydroxy-4-mercaptobiphenyl ( $HO-(C_6H_4)_2-SH$ ; HO-MBP).*

Single crystalline Si-doped n-type GaAs [100] wafers with a doping ratio of  $2.2 - 3.4 \times 10^{18} \text{ cm}^{-3}$  were purchased from American Xtal Technology Inc. (Fremont, California, USA). To improve the accuracy of the spectroscopic studies, an undoped GaAs layer of 100 nm thickness was grown on top by molecular beam epitaxy (MBE). For electrochemical measurements, an Ohmic contact was established at the backside of the wafer by electron beam vapor deposition of Ni (100 Å), Ge (200 Å), and Au (2500 Å).

The 4'-substituted-4-mercaptobiphenyl ( $X-(C_6H_4)_2-SH$ ; X-MBP) (*Fig. 3.1*) consist of a more rigid and bulkier biphenyl backbone (cross sectional area:  $21 \text{ \AA}^2$  (Ulman '01))

compared to the alkyl chains ( $18 \text{ \AA}^2$  (Nyburg & Lüth '72)). Synthesis of X-MBPs were reported elsewhere (Kang et al. '98; Sabatani et al. '93). The 4-mercaptobiphenyl ( $\text{H}-(\text{C}_6\text{H}_4)_2\text{-SH}$ ; H-MBP) was provided by W. Eck (University of Heidelberg, Germany), while 4'-methyl-4-mercaptobiphenyl ( $\text{CH}_3-(\text{C}_6\text{H}_4)_2\text{-SH}$ ;  $\text{CH}_3\text{-MBP}$ ) and 4'-hydroxy-4-mercaptobiphenyl ( $\text{HO}-(\text{C}_6\text{H}_4)_2\text{-SH}$ ; HO-MBP) were synthesized by A. Ulman (Polytechnic University of Brooklyn, NY, USA).

As an electrolyte a 10 mM phosphate buffer with 10 mM NaCl (pH = 7.5) was used. All the other chemicals were purchased from Sigma-Aldrich (München, Germany) and used without further purification. Freshly deionized ultra pure water (Millipore, Molsheim, France) was used throughout this study.

### 3.2 Preparation

The coating of GaAs with thiolates is a self-assembling process, where the sulfide covalently binds to surface arsenide (*Chapter 5.3.2*). *Figure 3.2* shows a sketch of the well-ordered 4'-substituted-4-mercaptobiphenyls (X-MBP) SAM on stoichiometric GaAs [100] surface.

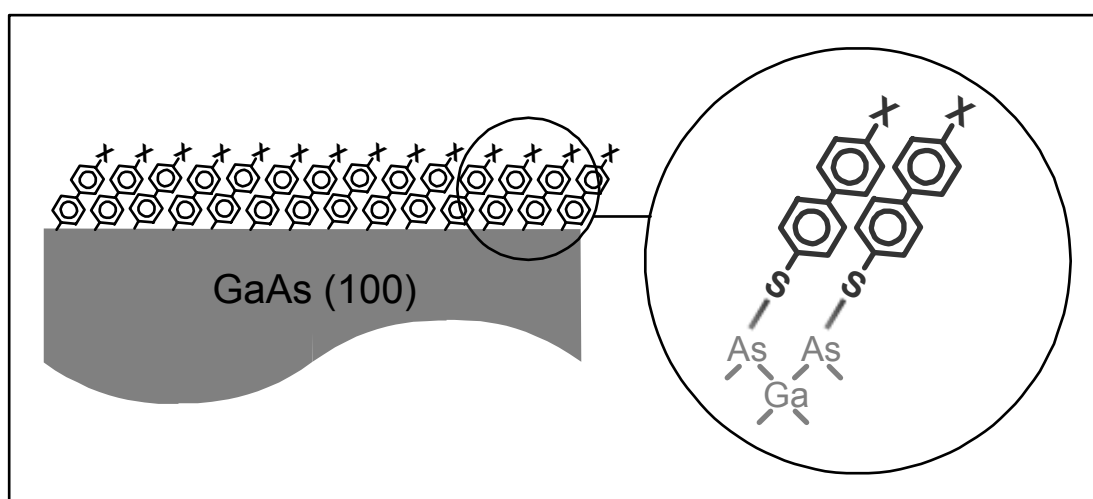


**Figure 3.2**

*Sketch of well-ordered 4'-substituted-4-mercaptobiphenyl (X-MBP) self-assembled monolayer (SAM) on stoichiometric GaAs [100] surface.*

Prior to the surface modification, the samples were sonicated in acetone for 3 min and rinsed with ethanol. The native oxide of GaAs was stripped by soaking the sample in concentrated HCl for 1 min, resulting in a stoichiometric GaAs [100] surface (Adlkofer & Tanaka '01; Adlkofer et al. '00; Stocker & Aspnes '82; Tufts et al. '90; Wagner et al. '78). SAMs were deposited by immersing freshly prepared substrates into 0.1 mM X-MBP solution in dimethylformamid (DMF), toluene and ethanol at different temperatures for 20 h to optimize the grafting conditions (*Chapter 4*). The reactions were carried out under nitrogen ( $N_2$ ) atmosphere to avoid surface oxidation (*Fig. 3.3*). After deposition, the sample was taken out from the reactor, sonicated for 1 min in ethanol, and dried by a  $N_2$  flow.

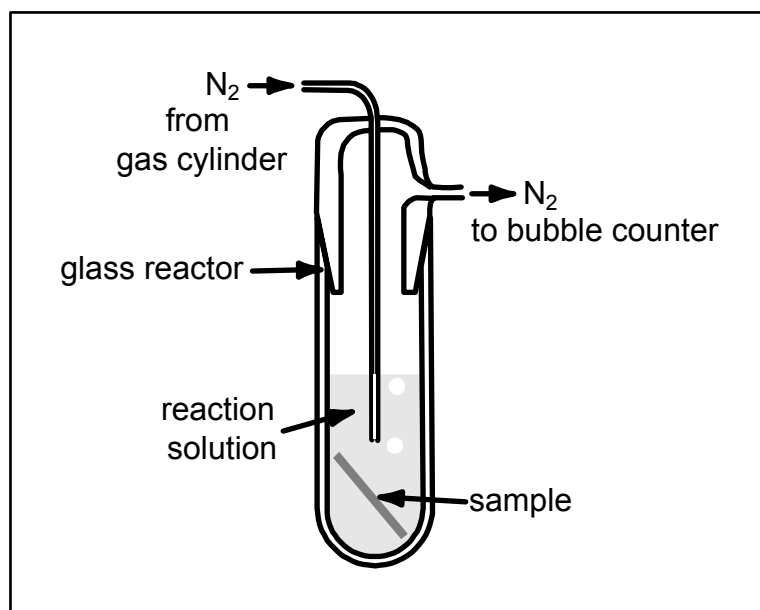


**Figure 3.3**

*Glass reactor for the deposition of 4'-substituted-4-mercaptobiphenyl (X-MBPs) self-assembled monolayers (SAMs).*

### **3.3 Measurement Methods**

Various surface sensitive techniques have been applied to analyze the gallium arsenide (GaAs) surface after the etching and grafting of the self-assembled monolayers (SAMs) of 4-mercaptobiphenyl (H-MBP), 4'-methyl-4-mercaptobiphenyl (CH<sub>3</sub>-MBP) and 4'-hydroxy-4-mercaptobiphenyl (HO-MBP).

The topography of the freshly etched (FE) and monolayer-coated surfaces was characterized by atomic force microscopy (AFM). The thickness of the deposited monolayer was determined by ellipsometry. The orientation of the H-MBPs on the GaAs surface was evaluated by near edge x-ray adsorption fine structure (NEXAFS) spectroscopy and chemical composition of the surfaces was determined by high resolution x-ray photoelectron spectroscopy (HRXPS). Total surface free energies and their dispersive and polar components were quantitatively determined by contact angle measurements. The drastic depression of oxidation and reduction by the H-MBP monolayer was monitored by cyclic voltammetry. Electrochemical properties of GaAs/electrolyte and GaAs/X-MBP/electrolyte interfaces were determined by impedance spectroscopy.

#### **3.3.1 Atomic Force Microscopy**

AFM is a convenient technique for topography measurements of bare and monolayer coated solids. The setup is schematically given in *Figure 3.4*. Two modes of operation are available, the contact and the tapping mode. In the contact mode the tip is always in contact with the sample and the aberration of the tip is adjusted by the piezo. In the tapping mode the tip oscillates near its resonance frequency. In close vicinity of the surface the amplitude is damped to an appointed value which is balanced by the piezo keeping the distance to the surface constant.

Topography of the freshly etched (FE) and the three 4'-substituted-4-mercaptobiphenyl (X-MBP) coated surfaces were characterized by AFM (Nanoscope IIIa, Digital Instruments, Mannheim, Germany). A silicon cantilever with a spring constant of about 40 N/m was used to scan an area of 1  $\mu\text{m}^2$  and 25  $\mu\text{m}^2$  in tapping mode. Typical modulation amplitudes and frequencies were in the order of 10 nm and 300 kHz, respectively.

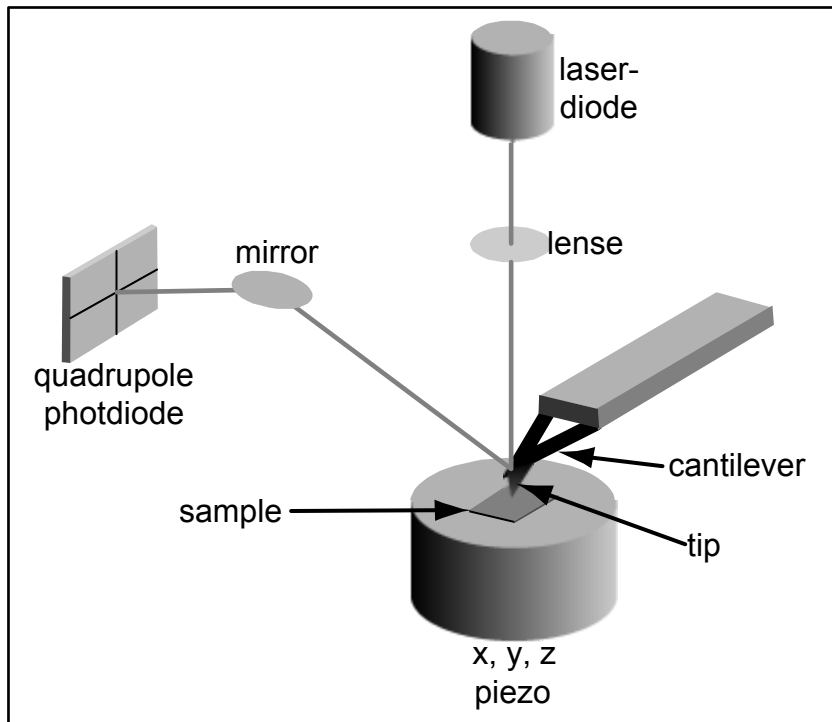


**Figure 3.4**

*The sample is moved relatively to the tip by the piezo. The movement of the cantilever mounted tip results in a change of the laser beam reflection which is monitored by the quadrupole diode.*

### 3.3.2 Ellipsometry

Ellipsometry is a non-invasive technique for thickness measurements of thin films. By using substrates with well defined values of the complex refractive indices, a thickness resolution of 1 Å can be reached. The incident beam with well defined polarization state is reflected at a sample and a rotating analyzer detects the change in polarization in terms of the two ellipsometric angles,  $\Psi$  and  $\Delta$  (Fig. 3.5).

By the following equation:

$$\frac{R_p}{R_s} = \tan \Psi \exp(-i\Delta) \quad (3.1)$$

the ratio between the complex reflection coefficients,  $R_p/R_s$ , for p- and s-polarized (parallel and perpendicular to the plane of incidence) light can be calculated.

Absolute values of the thickness or the refractive index of adsorbed layers can be determined by analyzing the ratio  $R_p/R_s$  in terms of Fresnel's equations.

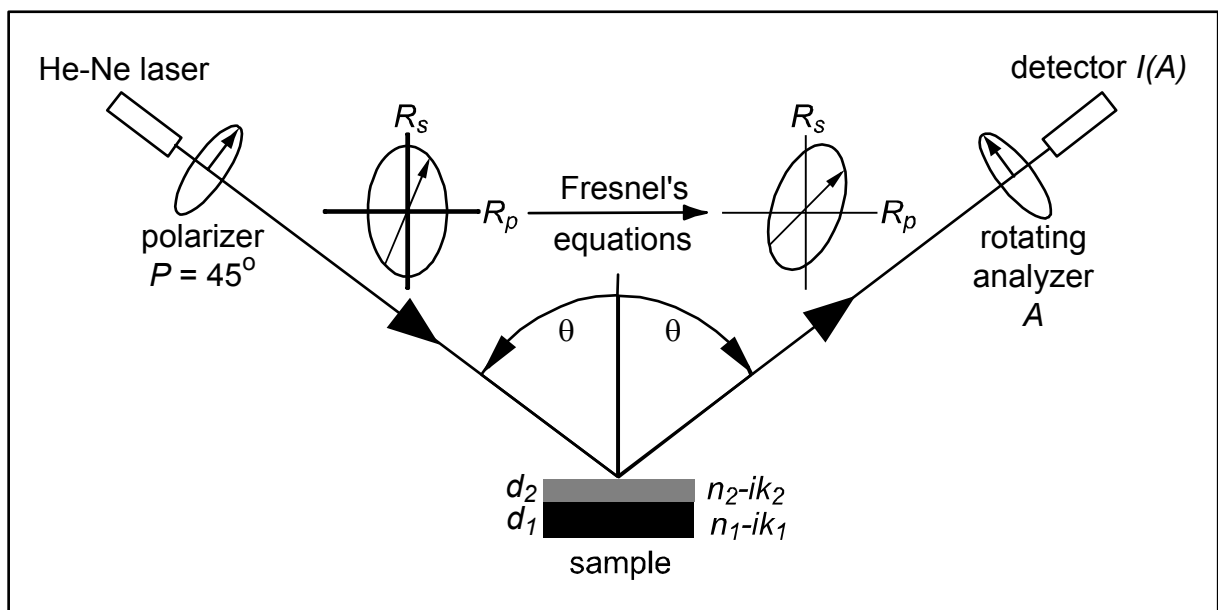


**Figure 3.5**

*Principle of ellipsometry.*

The measurements were carried out by using a conventional rotating analyzer ellipsometer (Plasmos GmbH Prozesstechnik, München, Germany) which consist of a HeNe laser (wavelength  $\lambda = 632.8$  nm, diameter  $\approx 0.5$  mm) and a polarizer as a

source for linear polarized light ( $P = 45^\circ$ ). From the bulk refractive index of GaAs substrates,  $n - ik = 3.856 - i0.196$  (Hellwege '83; Palik '85), the Brewster angle of the GaAs substrates can be obtained to be  $\beta = \arctan n = 75^\circ$ . In order to reach a good thickness resolution an angle of incidence,  $\theta = 70^\circ$  which is close to the Brewster angle was chosen for the measurements.

To take statistical values for the background data and the layer thickness the samples were measured at three different points before and after 4'-substituted-4-mercaptobiphenyl (X-MBP) monolayer deposition. Using the refractive index of biphenyl,  $n = 1.588$  (Weast '70), the thickness of the monolayer was estimated.

### **3.3.3 Spectroscopic Techniques**

Detailed information about the orientation of molecules and the chemical composition on the surface can be obtained by synchrotron-based near edge x-ray absorption fine structure (NEXAFS) spectroscopy and high resolution x-ray photoelectron spectroscopy (HRXPS).

Both the HRXPS and NEXAFS spectroscopy experiments were performed at room temperature and at a pressure of  $< 2 \times 10^{-9}$  mbar. The time for either the NEXAFS or HRXPS characterization was selected as a compromise between the spectra quality and the damage induced by x-rays (Heister et al. '01b; Jäger et al. '97; Wirde et al. '97; Zharnikov & Grunze '02).

#### **3.3.3.1 Near Edge X-Ray Fine Structure Spectroscopy**

The near edge x-ray absorption fine structure (NEXAFS) measurements to analyze the orientation of the grafted molecules were performed at the HE-SGM beamline of the synchrotron storage ring BESSY II in Berlin, Germany. The spectra acquisition was carried out at the C 1s absorption edge in the partial electron yield mode with a retarding voltage of  $-150$  V. Linear polarized synchrotron light with a polarization factor of 92% was used. The energy resolution was about 0.40 eV. The incident angle of the light was varied from  $90^\circ$  ( $E$ -vector in surface plane) to  $20^\circ$  ( $E$ -vector near surface normal) in steps of  $10^\circ - 20^\circ$  to monitor the orientational order of the 4-mercaptobiphenyl (H-MBP) molecules within the monolayer (Shaporenko et al. '03). This approach is based on so-called linear dichroism in x-ray absorption, i. e. the strong dependence of the cross-section of the resonant photoexcitation process on the orientation of the electric field vector of the linearly polarized light with respect to the molecular orbital of interest (Stöhr '92). The raw NEXAFS spectra were normalized to the incident photon flux with a spectrum of a clean, freshly sputtered gold sample. Before the normalization, a spectrum of freshly etched GaAs was subtracted from the raw spectrum of 4-mercaptobiphenyl coated GaAs (Frey et al. '00; Zharnikov et al. '00). The energy scale was referenced to the pronounced  $\pi_1^*$  resonance of highly oriented pyrolytic graphite at 285.35 eV (Batson '93).

### 3.3.3.2 High Resolution X-Ray Photoelectron Spectroscopy

The chemical composition of molecules on the surface can be derived by applying synchrotron-based high resolution x-ray photoelectron spectroscopy (HRXPS). This method involves irradiation of solids in vacuum with monoenergetic soft x-rays of the photon energy  $h\nu$  and sorting the emitted photoelectrons by their kinetic energy  $E_{kin}$  (Fig. 3.3) (Wagner et al. '78). The spectrum obtained by the analyzer is a plot of the number of emitted photoelectrons per energy interval versus their binding energy  $E_b$ , which can be described as

$$E_b = h\nu - E_{kin} \quad (3.2)$$

The choice of photon energy  $h\nu$  for every individual spectrum was based on the optimization of the photoionization cross-section for the corresponding core level (Band et al. '79; Goldberg et al. '81; Yeh & Lindau '85) as well as on adjustment of either surface or bulk sensitivity. The energy resolution was better than 100 meV, which allows to distinguish between different chemical species and to decompose the spectra into the respective components.

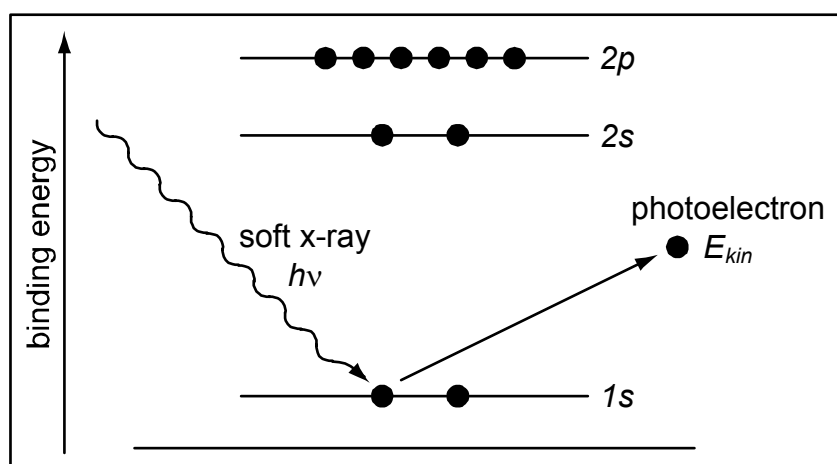


**Figure 3.6**

*Principle of x-ray photoelectron process.*

The HRXPS measurements were performed at the synchrotron storage ring MAX II at MAX-Lab in Lund, Sweden, using the D1011 and I311 beamlines. Both beamlines

are equipped with a Zeiss SX-700 plane-grating monochromator and a two-chamber UHV experimental station with a SCIENTA analyzer.

Excitation energies  $h\nu$  of 130 eV were used for measurements of the As 3*d* narrow scan spectra of the untreated (UT), the freshly etched (FE), and the three 4'-substituted-4-mercaptobiphenyl (X-MBP) coated GaAs. Photon energies  $h\nu$  in the range of 200 to 350 eV were used to scan the S 2*p* spectra of the three X-MBP coated GaAs samples. Energy calibration was performed individually for every spectrum to avoid effects related to the instability of the monochromator. The energy scale was referenced to the pronounced Au 4*f* "bulk" peak (83.93 eV) of a C12/Au sample (Heister et al. '01b).

The spectra were fitted using Voigt peak profiles and a Shirley background. The high energy resolution of the HRXPS and the domination of the As 3*d* spectra by a single doublet enable the decomposition of the parameters (fwhm = 0.65 eV, spin-orbit splitting = 0.69 eV, and branching ratio = 3/2) of the doublets, which were used as elementary fitting units. The decomposition was carried out self-consistently over the entire set of the spectra and the assignments of the individual emissions were performed in accordance with literature values (Adlkofer & Tanaka '01; Adlkofer et al. '00; Asai et al. '93; Chang et al. '91; Lunt et al. '91; Mao et al. '91; Moulder et al. '92; Shin et al. '91; Wagner et al. '78). The binding energies  $E_b$  of the individual doublets in the As 3*d* spectra are 41.1 eV (GaAs), 41.8 eV (elemental As, As<sup>0</sup>) and 42.4 eV (As-S). Within the fitting procedure, only the spectral features with visible individual components (doublets) were decomposed, whereas the broad, structure-less maxima, related to As oxides, were not considered. The resulting accuracy of the binding energies ( $E_b$ ) and fwhm's reported here is 50 meV. These values are noticeably higher than the ultimate accuracy of the experimental setup (Heister et al. '01a), which is based on the distribution of the resulting fit parameters over the spectra of different samples in the same spectral region.

### 3.3.4 Contact Angle Measurement

Total surface free energies of bare or coated surfaces and their dispersive and polar components can quantitatively be estimated by contact angle measurements.

The contact angles between solid surfaces and liquids can be measured by forming a sessile drop (volume  $\sim 10 \mu\text{L}$ ) at the end of a blunt-ended needle and placing it on the substrates. In our study, a G10 contact angle meter (Krüss GmbH, Hamburg, Germany) equipped with a CCD camera was used and the measurements were carried out in an ambient atmosphere at room temperature. The advancing contact angles of water were determined during the continuous growth of a droplet, while the receding angles of water were measured during the volume reduction by suction. The angle between the droplets and the substrate was determined with the aid of DSA1 droplet shape analysis program (Krüss GmbH, Hamburg, Germany) with an accuracy of  $\pm 2^\circ$ . Based on Owens-Wendt method (Owens & Wendt '69), the total surface free energy  $\gamma$ , as well as the dispersive  $\gamma_s$ , and polar  $\gamma_p$ , components were evaluated, using the static contact angles of water, diiodomethane, and glycerol and their surface free energies given in *Table 3.1*.

The overall accuracy throughout the evaluation of surface free energies of the samples was within  $\pm 3 \text{ mNm}^{-1}$ .

liquid	total surface free energy $\gamma$ [ $\text{mNm}^{-1}$ ]	dispersive component $\gamma_s$ [ $\text{mNm}^{-1}$ ]	polar component $\gamma_p$ [ $\text{mNm}^{-1}$ ]
water	72.8	26	46.8
diiodomethane	50.8	44.1	6.7
glycerol	64	34	30

**Table 3.1**

*Total surface free energies  $\gamma$ , dispersive components  $\gamma_s$ , and polar components,  $\gamma_p$  of water, diiodomethane and glycerol. Taken from the DSA1 droplet shape analysis program (Krüss GmbH, Hamburg, Germany).*

### 3.3.5 Electrochemical Measurements

Electrochemical properties of the freshly etched (FE) and the 4'-substituted-4-mercaptobiphenyl (X-MBP) coated GaAs were systematically characterized by cyclic voltammetry and impedance spectroscopy (VoltaLab 40, Radiometer Copenhagen) at room temperature.

The contact area of the surface to the electrolyte was  $0.28 \text{ cm}^2$ , and the volume inside the chamber was about 1.5 ml. A Ag/AgCl electrode (Metrohm, Herisau, Switzerland) was used as reference electrode, and a Au electrode as the counter electrode. Throughout this study, the potential,  $U(t)$ , was applied versus the Ag/AgCl electrode. Instead of using rotating disk electrodes (Hens & Gomes '99; Menezes & Miller '83; Uhlendorf et al. '95), a constant flow of the electrolyte was applied to the measuring chamber (Fig. 3.7).

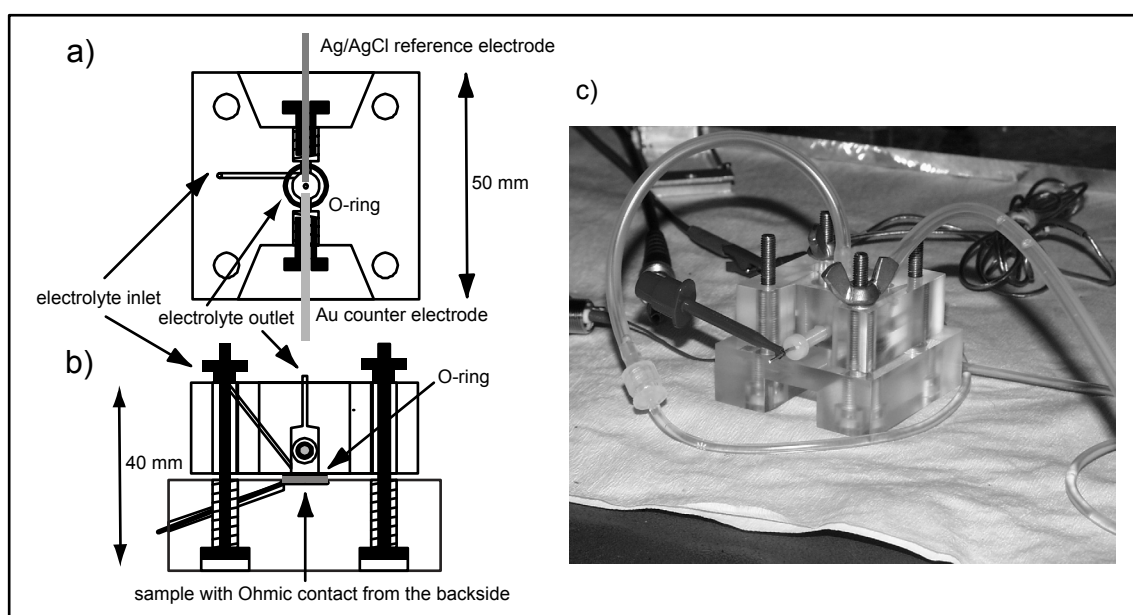


**Figure 3.7**

*Measuring chamber for the electrochemical studies:*

*a) top view*

*b) side view*

*c) appearance*

### 3.3.5.1 Cyclic Voltammetry

Electrochemical processes across the interface can be studied by cyclic voltammetry. In this method, the current response,  $I(U)$ , was monitored as a function of the applied potential,  $U(t)$  (Fig. 3.8). Electrochemical processes across the interface, i.e. charge transfer, adsorption, and dissolution, can be determined by the shape and shift of the cyclic voltammograms (Bard & Faulkner '80).

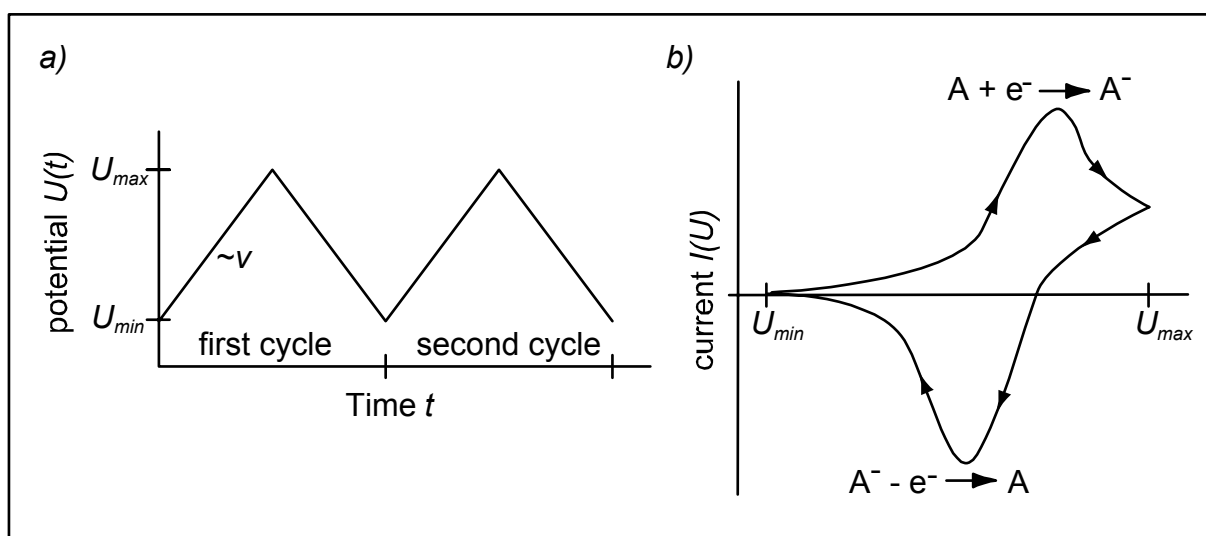


**Figure 3.8**

a) Cyclic potential sweep.

b) Resulting cyclic voltammogram of reversible charge transfer.

Unfortunately, the GaAs/electrolyte interfaces near neutral pH conditions are suffering from coupled and consecutive electrochemical processes, such as (1) reduction of an oxidant, (2) oxidation of a reductant, (3) surface passivation by film formation, (4) substrate dissolution by external current, and (5) substrate dissolution by hole injection of an oxidant (Menezes & Miller '83). Thus, only qualitative information is available from cyclic voltammetry.

In this study, five cycles were measured for freshly etched and 4-mercaptobiphenyl (H-MBP) coated GaAs interfaces in the potential range from  $-1000$  mV to  $+500$  mV at a scan speed of  $v = 25$  mV s $^{-1}$ .

### 3.3.5.2 Impedance Spectroscopy

Electrochemical properties of bare and coated substrate/electrolyte interfaces can be characterized by impedance spectroscopy (Macdonald '87).

In this method, a sinusoidal potential  $U(t) = U_{bias} + U_0 \sin(\omega t)$  with a bias potential  $U_{bias}$ , frequency  $\omega$ , and amplitude  $U_0$  is applied across the interface, and the current response  $I(t) = I_0 \sin(\omega t + \varphi(\omega))$  is monitored.

To consider the relationship between two related sinusoidal signals,  $U(t)$  and  $I(t)$ , each can be represented as a phasor,  $\hat{U}$  and  $\hat{I}$ , rotating at the same frequency  $\omega$ . Generally, they are not in phase, therefore their phasors will be separated by the phase angle,  $\varphi$  (Fig. 3.9).

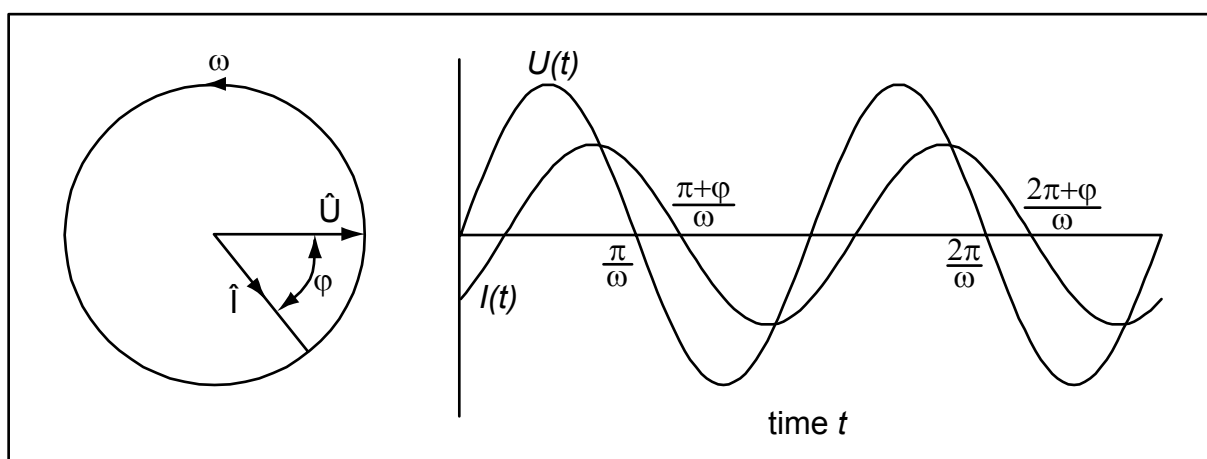


**Figure 3.9**

*Relationship between potential and current signals at frequency  $\omega$ .*

The generalized version of Ohm's law

$$\hat{U} = \hat{I}Z \quad (3.3)$$

links the potential to the current through a complex resistance  $Z = R - iX$ , called impedance.

The absolute value of  $Z$  is given by

$$|Z| = \sqrt{R^2 + X^2} \quad (3.4)$$

and the phase angle is

$$\tan \varphi = \frac{R}{X} \quad (3.5)$$

Thus, in the polar form, the complex impedance  $Z$  can be represented as:

$$Z = |Z| e^{i\varphi} \quad (3.6)$$

The impedance spectra can be fitted by using equivalent circuit models. These models consist of resistors and capacitors, which represent the individual electrochemical properties of the interface.

In general, a GaAs/electrolyte interface can be represented by the equivalent circuit given in *Figure 3.10* proposed by Allongue et al. (Allongue & Catchet '85; Horowitz et al. '84).

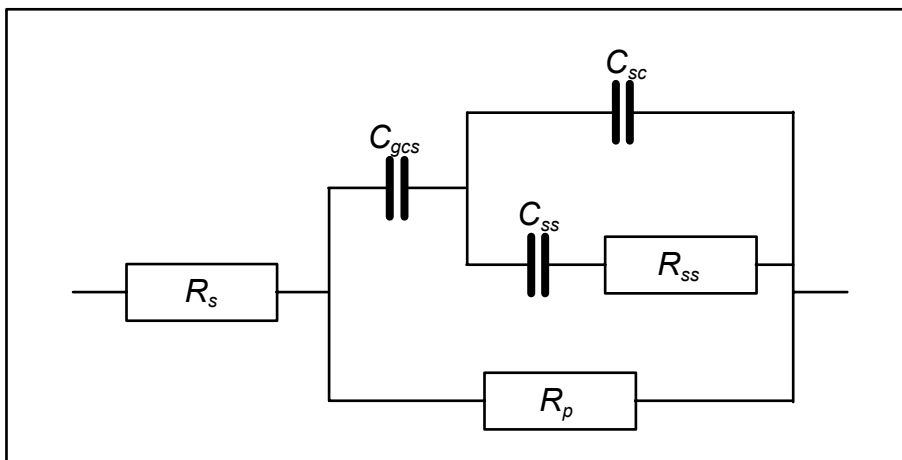


**Figure 3.10**

*Equivalent circuit model of GaAs/electrolyte interface proposed by Allongue et al. (Allongue & Catchet '85; Horowitz et al. '84).*

The serial resistance  $R_s$  corresponds to the Ohmic behavior of electrolytes and contacts, while the parallel resistance  $R_p$  is attributed to an Ohmic behavior of the interface.  $C_{ss}$  and  $R_{ss}$  denote the capacitance and resistance of the surface states.  $C_{sc}$  is the capacitance of the semiconductor space charge region, and  $C_{gcs}$  is the capacitance of Gouy-Chapmann-Stern layer (Bard & Faulkner '80). Our preliminary

fitting (Adlkofer & Tanaka '01; Adlkofer et al. '00) showed that it was impossible to estimate the contributions from the surface states quantitatively, which might be attributed to the relative low density of the surface states (Allongue & Catchet '85; Horowitz et al. '84). Consequently, the impedance spectra was analyzed according to the simplified equivalent circuit model depicted in *Figure 3.11*, where capacitance  $C$  represents the complex interface capacitance and which is used in this study (Adlkofer & Tanaka '01; Adlkofer et al. '00). The impedance  $Z$  of this circuit model is calculated by:

$$Z(\omega) = |Z(\omega)| e^{i\phi(\omega)} = R_s + \frac{(R_p - i2\pi\omega CR_p)^2}{1 + (2\pi\omega CR_p)^2} \quad (3.7)$$

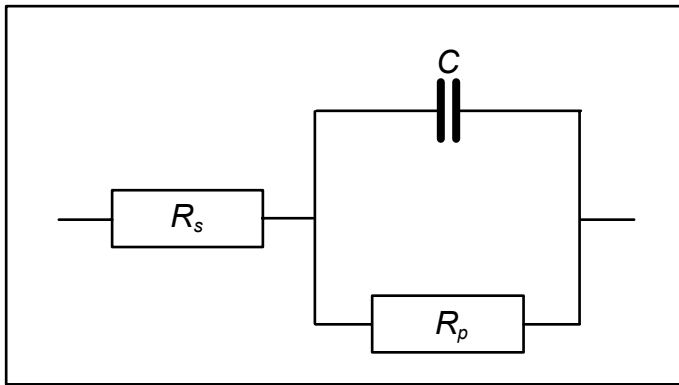


**Figure 3.11**

*Simplified equivalent circuit model used in this study.*

For the freshly etched surface, the interface capacitance  $C$  can be explained as the serial connection of  $C_{gcs}$  and capacitance of the semiconductor space charge region  $C_{sc}$ :

$$C = \frac{C_{sc} C_{gcs}}{C_{sc} + C_{gcs}} \quad (3.8)$$

$C_{gcs}$  can be divided into the contribution from Helmholtz layer  $C_h$  and that from the diffuse layer  $C_{diff}$ .

$$C_{gs} = \frac{C_h C_{diff}}{C_h + C_{diff}} \quad (3.9)$$

As  $C_h \geq 140 \mu\text{Fcm}^{-2}$  and  $C_{diff} \geq 0.9 \text{ Fcm}^{-2}$  in our experimental system (Bard & Faulkner '80), these contributions could be omitted. Hence, the capacitance of the space charge region is the major contribution to the complex interface capacitance  $C$  (Adlkofer & Tanaka '01; Adlkofer et al. '00).

Impedance spectra of freshly etched and the three X-MBP coated GaAs and were taken between 50 kHz and 1 MHz under sinusoidal potentials with an amplitude of  $U_0 = 10 \text{ mV}$ . To estimate the electrochemical parameters quantitatively from the measured impedance data, the whole system was represented by simple ideal elements of a simplified equivalent circuit model composed of serial resistance  $R_s$ , interface capacitance  $C$ , and interface resistance  $R_p$  (Fig. 3.11). The fitting was done by a self-written program and the errors through the data analysis were kept below 10 %. The spectra were presented by the Bode plot of the absolute value  $|Z(\omega)|$  and the phase  $\varphi(\omega)$  of the impedance as a function of the frequency  $\omega$ .

## 4 Optimization of Grafting Conditions

The quality of the self-assembled monolayer (SAM) of the 4'-substituted-4-mercaptobiphenyl (X-MBP) on GaAs strongly depends on the grafting conditions (solvent, concentration, reaction time and temperature). Impacts of solvents were firstly examined by carrying out the grafting reaction of 4-mercaptobiphenyl (H-MBP) in three different solvents (dimethylformamid, toluene, ethanol) at 20 °C for 20 h. The quality of the resulted SAMs was obtained by measuring the ellipsometric thickness  $d$  and the interface resistance  $R_p$  immediately after the grafting ( $t = 0$  h) and after 2 h ( $t = 2$  h) by impedance spectroscopy. At the next step, the monolayers prepared at different reaction temperatures, i.e. 20 °C, 35 °C, and 50 °C were compared. These results gave the optimal grafting conditions 0.1 mM X-MBP in ethanol at 50 °C for 20 h used, in this study.

### 4.1 Impact of Solvents

The surface characteristics of the surfaces prepared by three different solvents (dimethylformamid (DMF), toluene and ethanol) at 20 °C are summarized in *Table 4.1*.

solvent	ellipsometric thickness $d$ [Å]	Interface resistance $R_p$ at $t = 0$ h [ $M\Omega\text{cm}^2$ ]	Interface resistance $R_p$ at $t = 2$ h [ $M\Omega\text{cm}^2$ ]
DMF	2	0.61	1.3
toluene	6	1.3	1.9
ethanol	6	1.6	2.1

**Table 4.1**

*4-mercaptobiphenyl (H-MBP) layers were grafted in dimethylformamid (DMF), toluene, and ethanol at 20 °C. for 20 h. Ellipsometric thickness  $d$ , interface resistance  $R_p$  shortly after grafting ( $t = 0$  h), and after 2 h ( $t = 2$  h) measured by impedance spectroscopy. Note that all the layers showed electrochemical instability monitored by impedance spectroscopy.*

As presented in the *Table*, the reaction in DMF resulted in a very poor coating, where the ellipsometric thickness was merely 2 Å. The interface resistance was increased

by a factor of 10 from that of freshly etched (FE) GaAs (*Chap 6.3:  $R_p(\text{FE}, t = 0 \text{ h}) = 64 \text{ k}\Omega \text{ cm}^2$* ), however, the impedance spectra were not stable. Using toluene and ethanol as solvents, the surface coverage was remarkably improved. Ellipsometric thickness amounted to 6 Å, and the interface resistance increased up to more than 1 MΩcm<sup>2</sup>. The instability in impedance spectra could still be observed, but the drift was much smaller in comparison to the one prepared in DMF. Based on the highest interface resistance obtained, we chose ethanol as the solvent. Nevertheless, the impedance spectra of the sample prepared in ethanol showed a clear instability. The concentration of H-MBP (e.g. 1 mM) as well as the reaction time (e.g. 40 h) was increased, but these often resulted in heterogeneous and obviously too thick layers ( $d > 16 \text{ Å}$ ), suggesting the formation of multilayers.

## 4.2 Impact of Temperature

At the next step, the 4-mercaptobiphenyl (H-MBP) monolayers prepared in ethanol at different reaction temperatures, i.e. 20 °C, 35 °C, and 50 °C were compared (*Table 4.2*). The samples coated at 20 °C and at 35 °C did not exhibit any clear differences in ellipsometric thickness (5, 6 Å), and showed similar shifts in interface resistance  $R_p$  from approx. 1.7 to 2.1  $M\Omega\text{cm}^2$  in 2 h. On the other hand, the sample prepared at 50 °C showed clear increase in thickness (10 Å) and in the interface resistance, 3.2  $M\Omega\text{cm}^2$ . In fact, this resistance remained stable for more than 20 h, as presented in *Chapter 6.3*. Noticeable, further increasing the preparation temperature to 60 °C did not increase the quality of the layer.

temperature $T$ [°C]	ellipsometric thickness $d$ [Å]	interface resistance $R_p$ at $t = 0$ h [ $M\Omega\text{cm}^2$ ]	interface resistance $R_p$ at $t = 2$ h [ $M\Omega\text{cm}^2$ ]
20	6	1.6	2.1
35	5	1.8	2.0
50	10	3.2	3.2

**Table 4.2**

*Effects of reaction temperature on ellipsometric thickness  $d$ , and interface resistance  $R_p$  at  $t = 0$  h and  $t = 2$  h. Here, the reactions were carried out in dry ethanol for 20 h. Although there were almost no differences between the samples prepared at r.t. and at 35 °C, the grafting at 50 °C resulted in an improved surface coating.*

These results gave the optimal grafting conditions 0.1 mM X-MBP in ethanol at 50 °C for 20 h, which were used for the following studies.

## 5 Structural Analysis in Dry States

Various surface sensitive techniques in dry states have been applied to analyze the gallium arsenide (GaAs) surface after the etching and grafting of the self-assembled monolayers (SAMs) of 4'-substituted-4-mercaptobiphenyl (X-MBP).

The surface topography was measured by atomic force microscopy (AFM). The thickness of the SAM was evaluated by ellipsometry. From near edge x-ray adsorption fine structure (NEXAFS) spectroscopic studies the tilt of the 4-mercaptobiphenyl (H-MBP) molecules was obtained. The covalent attachment of the sulfide to the surface arsenide was confirmed by high resolution x-ray spectroscopy (HRXPS).

### 5.1 Surface Topography

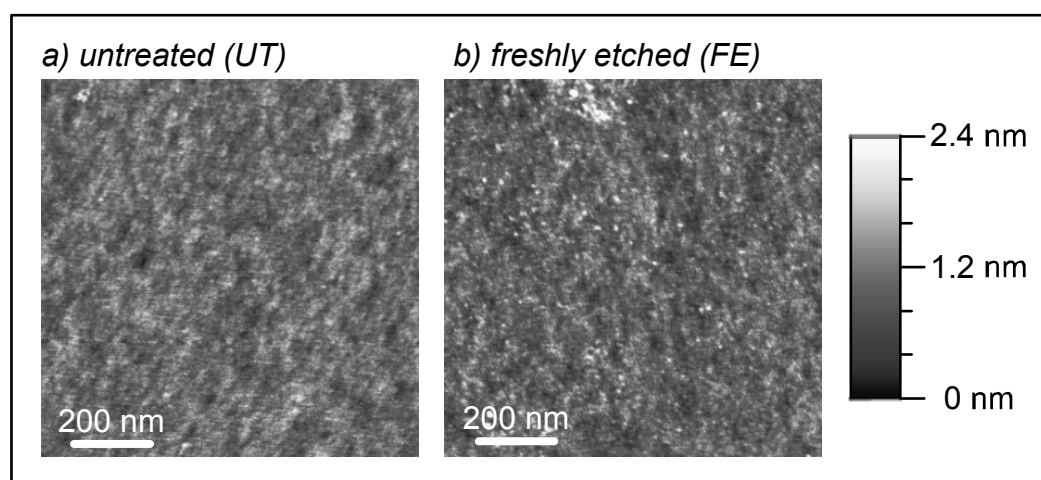


**Figure 5.1**

*Tapping mode AFM images of (a) untreated (UT, rms roughness 2.8 Å) and (b) freshly etched (FE, 3.3 Å) GaAs.*

Surface topography of a GaAs [100] substrate was characterized by atomic force microscopy (AFM) at several different locations within an area of  $1 \mu\text{m}^2$ . The untreated (UT) GaAs surface with native oxide showed a rms roughness of 2.8 Å (Fig. 5.1 a). The corresponding value after the HCl stripping was slightly increased to 3.3 Å (Fig. 5.1 b), suggesting the surface roughening due to wet chemical etching.

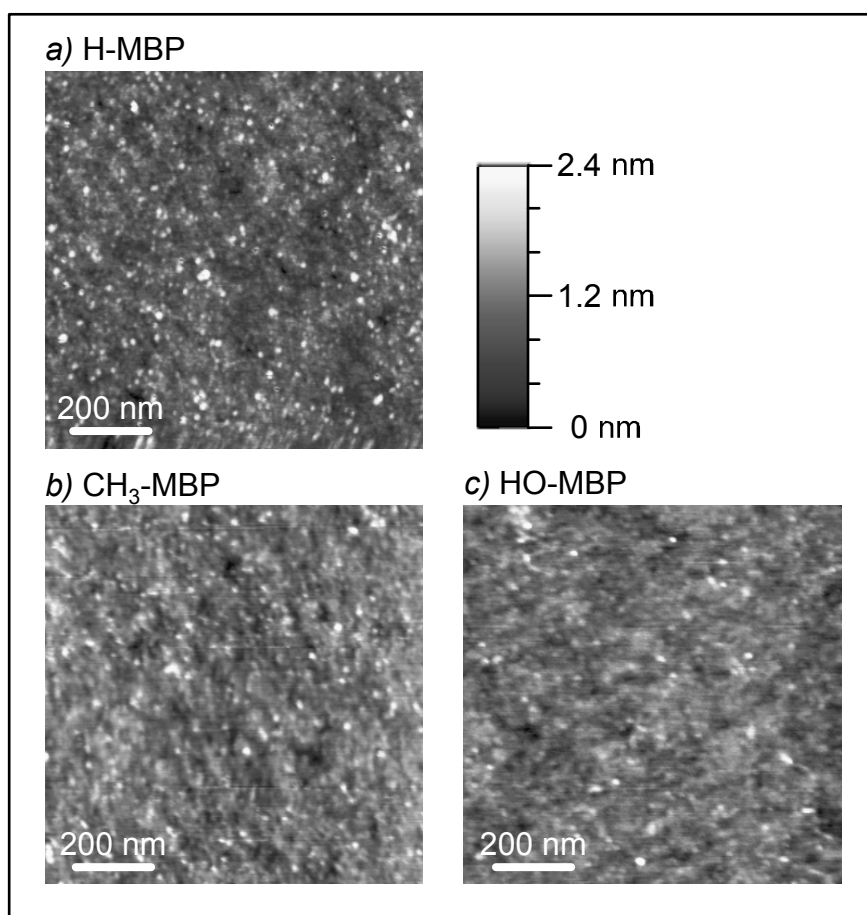


**Figure 5.2**

*Tapping mode AFM images of GaAs coated with*  
*a) 4-mercaptobiphenyl (H-MBP, rms roughness 3.5 Å),*  
*b) 4'-methyl-4-mercaptobiphenyl (CH<sub>3</sub>-MBP, 3.1 Å) and*  
*c) 4'-hydroxy-4-mercaptobiphenyl (HO-MBP, 2.7 Å).*

Figure 5.2 shows the tapping mode AFM images of GaAs coated with (a) 4-mercaptobiphenyl (H-MBP), (b) 4'-methyl-4-mercaptobiphenyl (CH<sub>3</sub>-MBP) and (c) 4'-hydroxy-4-mercaptobiphenyl (HO-MBP) monolayers. The rms roughness values within the scanned area were 3.5 Å for the GaAs with H-MBP (Fig. 5.2 a), 3.1 Å for the GaAs with CH<sub>3</sub>-MBP (Fig. 5.2 b) and 2.7 Å for the GaAs with HO-MBP (Fig. 5.2 c). The grafting reactions resulted in a rms roughness comparable to that of a freshly etched surface, i.e. that grafting reactions did not increase the surface roughness.

## 5.2 Film Thickness

The thicknesses of the 4'-substituted-4-mercaptobiphenyl (X-MBP) layers were determined by ellipsometry. A reproducible value of  $10 \pm 2$  Å was determined. This suggests the grafting of a monolayer. Experimental errors in the obtained thickness are mostly due to the chemical instability of the freshly etched GaAs, which makes the background measurements difficult. Nevertheless, it should be pointed out that the obtained ellipsometric parameters ( $\Psi$  and  $\Delta$ ) were reproducible after more than one week, confirming the chemical stability of the coated surface. There are several reports on the thickness of 4-mercaptobiphenyl (H-MBP) monolayer on gold measured by ellipsometry. For example, Tao et al. estimated the thickness of 9.4 Å (Tao et al. '97), while Kang et al. reported 14 Å (Kang et al. '01). It should be noted that both of these studies assumed the smaller refractive index of 1.462 for the monolayer, which is a typical value for alkyl chains (Lide '97). The refractive index of bulk biphenyl  $n = 1.588$  (Weast '70) was chosen for the analysis, which might result in a slightly different monolayer thickness. Previously, Geyer et al. determined an average tilt angle between the phenyl ring and the Au surface normal by near edge x-ray absorption fine structure (NEXAFS) spectroscopy of  $15 \pm 5^\circ$  (Geyer et al. '99). Thus, the deviation between the obtained thickness and the corresponding values on Au can be related either to (a) different refractive indices chosen for the data analysis, or to (b) different orientation of the biphenyl backbones on GaAs and on Au. The obtained thickness showed reasonable agreement with those reported on metal surfaces, suggesting the deposition of monolayers with a small tilt angle to the surface normal (*Chapter 5.3.1*).

### 5.3 Molecular Orientation and Chemical Composition

From near edge x-ray adsorption fine structure (NEXAFS) spectroscopy studies the molecular orientation of the 4-mercaptobiphenyl (H-MBP) was evaluated.

Changes in chemical composition of GaAs before and after grafting of 4'-substituted-4-mercaptobiphenyl (X-MBP) were studied by high resolution x-ray photoelectron spectroscopy (HRXPS).

#### 5.3.1 Molecular Orientation

The orientation of the 4-mercaptobiphenyl (H-MBP) molecules on the GaAs surface was measured with an aid of near edge x-ray adsorption fine structure (NEXAFS) spectroscopy.

The C 1s NEXAFS spectra of (*broken line*) freshly etched (FE) and (*solid line*) H-MBP coated GaAs taken at so-called magic angle of x-ray incidence ( $\theta = 55^\circ$ ) and divided by the spectrum of clean Au are presented in *Figure 5.3* (Shaporenko et al. '03).

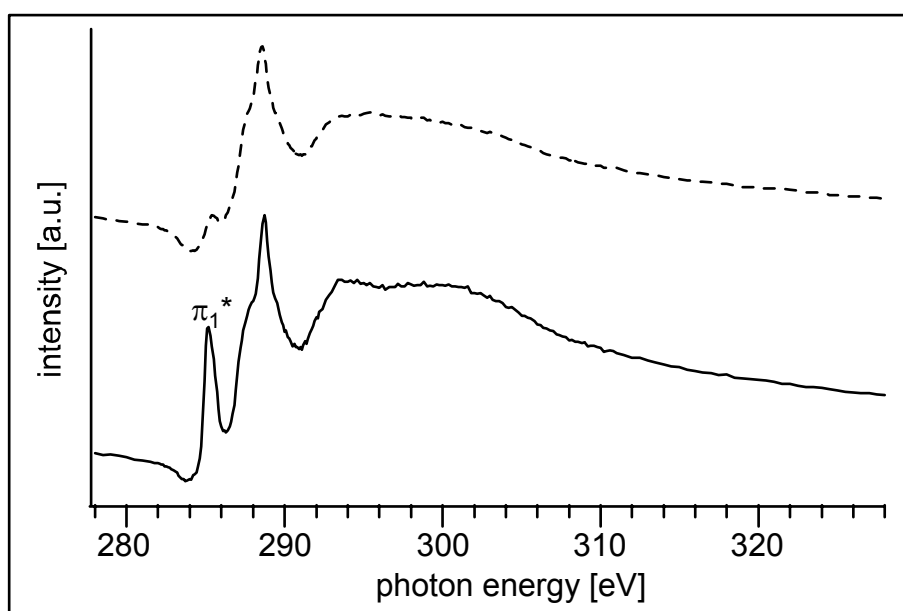


**Figure 5.3**

C 1s NEXAFS spectra of (*broken line*) freshly etched (FE) and (*solid line*) 4-mercaptobiphenyl (H-MBP) coated GaAs divided by the spectrum of clean Au. The spectra are acquired at an angle of x-ray incidence  $\theta = 55^\circ$ .

The spectra acquired at the magic angle exclusively reflect the electronic structure of the unoccupied molecular orbitals of the investigated films and are not affected by the angular dependence of the absorption cross-sections (Stöhr '92). The FE GaAs (*Fig. 5.3 broken line*) reveals an absorption structure, which can be related to carbon contamination in the near-surface region. The spectra of H-MBP coated GaAs (*Fig. 5.3 solid line*) exhibit additional absorption maxima, which are characteristic for intact aromatic rings. In particular, a distinct  $\pi_1^*$  resonance at a photon energy of 285.2 eV is dominant and the entire NEXAFS spectra exhibit a shape characteristic for self-assembled monolayers (SAMs) of aromatic compounds (Frey et al. '01; Fuxen et al. '01; Geyer et al. '99; Himmel et al. '98; Zharnikov & Grunze '01).

The normalized (*Chapter 3.3.3.1*) spectra of H-MBP coated GaAs for different incident angles of x-rays  $\theta$  are shown in *Figure 5.4* (Shaporenko et al. '03). Along with the  $\pi_1^*$  resonance, they reveal other characteristic absorption maxima of the carbon atoms in the H-MBP molecules (Frey et al. '01; Fuxen et al. '01; Geyer et al. '99; Himmel et al. '98; Zharnikov & Grunze '01), such as R\*/C-S\* resonances at photon energies of 287.25 eV and 287.75 eV (Horsley et al. '85; Stöhr & Outka '87; Weiss et al. '98), a  $\pi_2^*$  resonance at a photon energy of 288.9 eV (there is also an alternative  $\sigma^*(\text{CH})$  assignment for this resonance) (Agren et al. '95; Yokoyama et al. '90), and  $\sigma^*$  resonances at photon energies of  $\approx 293.0$  eV and  $\approx 300.0$  eV. The absorption edge is presumably located at a photon energy of  $\approx 287$  eV (Frey et al. '01; Geyer et al. '99; Himmel et al. '98).

As seen in *Figure 5.4*, the intensities of the  $\pi_1^*$  resonances vary strongly when the angle of incidence of the x-rays  $\theta$  is changed (Shaporenko et al. '03). The pronounced linear dichroism suggests a high orientational order for the H-MBP monolayers on GaAs. In addition, the increase in the  $\pi_1^*$  resonance intensity with increasing incident angle implies an upright orientation of the biphenyl moieties because the transition dipole moment of the  $\pi_1^*$  resonances is perpendicular to the ring plane.

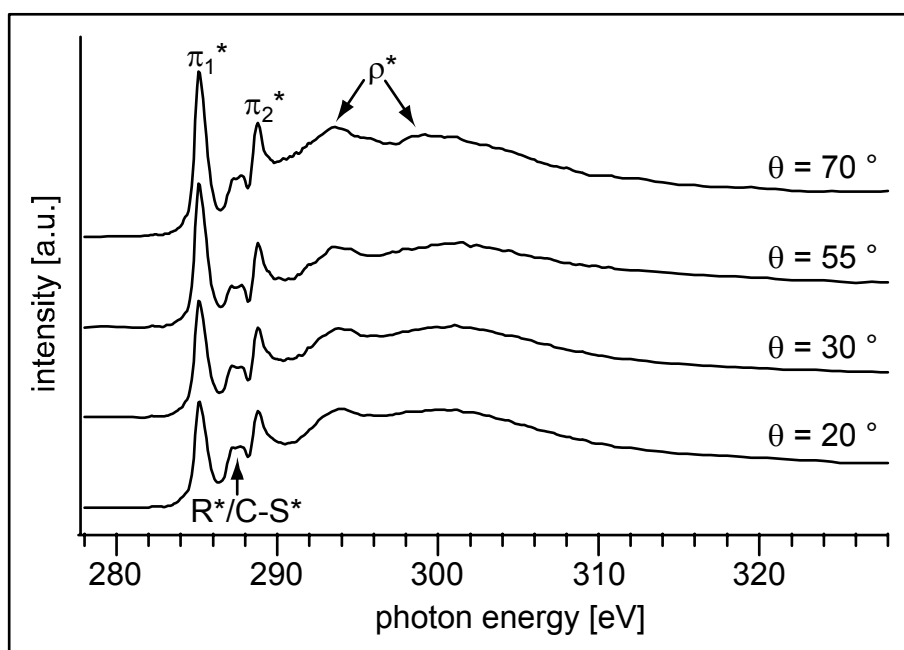


**Figure 5.4**

*Normalized C 1s NEXAFS spectra of a 4-mercaptobiphenyl coated GaAs sample acquired at angles of x-ray incidence  $\theta$  of 70°, 55°, 30°, and 20°.*

Additional for the qualitative conclusions on the orientational order in the H-MBP monolayer on GaAs, a value of the average tilt angle of the aromatic chains in these systems can be obtained by a quantitative analysis of the angular dependence of the NEXAFS resonance intensities (Stöhr '92). For this analysis, the  $\pi_1^*$  resonance was selected as the most intense and distinct resonance in the absorption spectra of H-MBP coated GaAs.

For the H-MBP, the intensity  $I$  of the  $\pi_1^*$  resonance is related to the average tilt angle  $\alpha$  of the  $\pi_1^*$  orbital with respect to the surface normal and the x-ray incidence angle  $\theta$  by (Stöhr '92)

$$I(\alpha) \propto 1 + \frac{1}{2} \cdot (3 \cdot \cos^2 \theta - 1) \cdot (3 \cdot \cos^2 \alpha - 1) \quad (5.1)$$

which is a standard expression for a vector-type orbital. The term  $\cos^2 \alpha$  in *Equation 5.1* can be expressed through the twist angle  $\vartheta$  of the aromatic rings with respect to the plane spanned by the surface normal and the molecular axis and through the average tilt angle  $\varphi$  of the molecular axis with respect to the surface normal by (Rong et al. '01)

$$\cos \alpha = \cos \vartheta \cdot \sin \varphi . \quad (5.2)$$

Here, a planar conformation of the biphenyl moieties (the dihedral angle is equal to zero) within the densely packed SAMs is assumed in accordance with literature data for crystalline biphenyl (Lii & Allinger '89) and thioaromatic self-assembled monolayers on Au (Himmel et al. '98).

Consequently, the average tilt angle  $\varphi$  of the molecular axis for a known twist angle  $\vartheta$  is defined by

$$I(\vartheta, \varphi) \propto 1 + \frac{1}{2} \cdot (3 \cdot \cos^2 \vartheta - 1) \cdot (3 \cdot \cos^2 \vartheta \cdot \sin^2 \varphi - 1) . \quad (5.3)$$

Assuming a herringbone arrangement of H-MBP molecules like in the aromatic SAMs on Au (Chang et al. '94; Dharani et al. '96; Himmel et al. '98), two different spatial orientations of the biphenyl moieties with reverse twist angles  $\vartheta_1 = -\vartheta_2$  and the same tilt angles  $\varphi_1 = \varphi_2$  were achieved. In this particular case, the contributions of each spatial orientation to the resonance intensity (*Eq. 5.3*) are the same and *Equation 5.3* can be used for the data evaluation without any modification.

To avoid normalization problems, the absolute intensities were not analyzed, but the intensity ratios  $I(\theta)/I(20^\circ)$ , where  $I(\theta)$  is the intensity of the  $\pi_1^*$  resonance at an x-ray incidence angle  $\theta$  (Stöhr '92; Stöhr & Outka '87). In addition, same twist angle  $\vartheta = 32^\circ$  for the biphenyl moieties in 4-mercaptobiphenyl monolayers on GaAs as found for thioaromatic bulk materials was assumed (Cruickshank '56; Kitaigorodskii '61; Trotter '61). This assumption is based on theoretical estimations for the molecular arrangements in biphenyl and naphthalene mercaptan films on Au (Chang et al. '94) and on the experimental data for a series of oligo(phenylethynyl)benzenethiols (Dharani et al. '96).

The results of the NEXAFS data analysis are presented in *Figure 5.5*, where the angular dependence of the  $\pi_1^*$  resonance intensity ratio  $I(\theta)/I(20^\circ)$  for H-MBP coated GaAs is depicted (Shaporenko et al. '03), along with theoretical dependencies (*solid and broken lines*) for several selected average tilt angles  $\varphi$  of the biphenyl moieties in the H-MBP film.

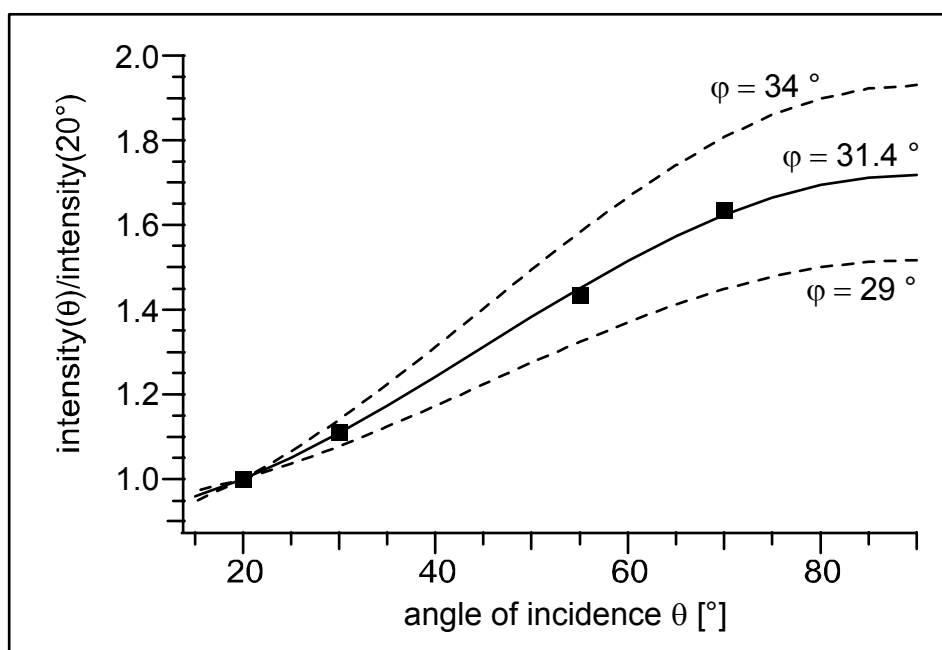


**Figure 5.5**

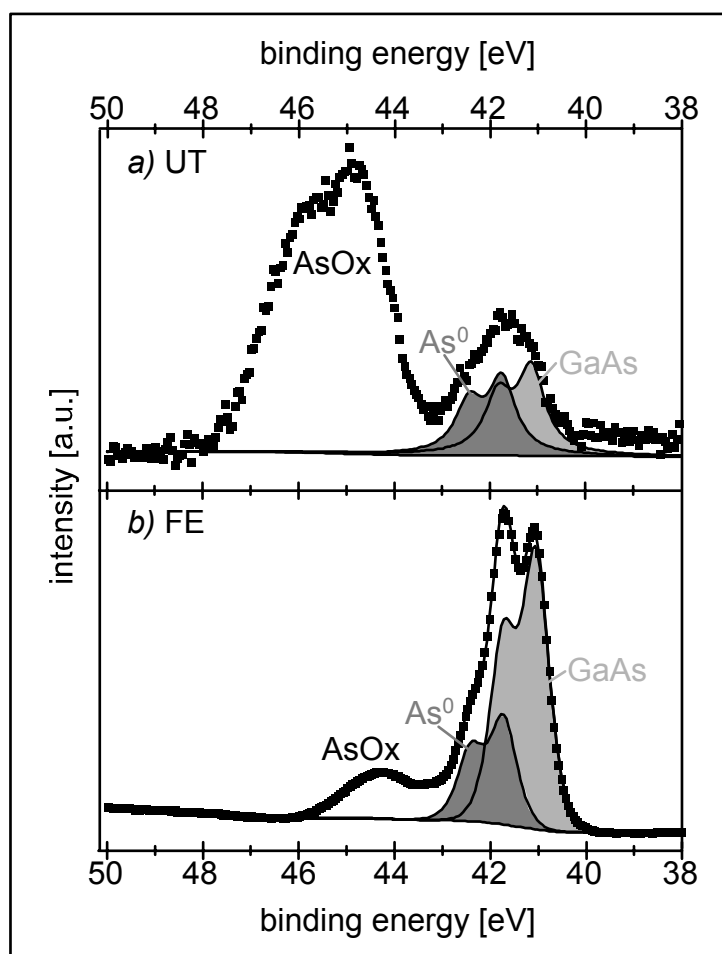
The angular dependencies of the  $\pi_1^*$  resonance intensity ratio  $I(\theta)/I(20^\circ)$  for a H-MBP coated GaAs sample. For comparison, the theoretical dependencies for two selected average tilt angles ( $\varphi = 35^\circ$  and  $\varphi = 29^\circ$ ) of the  $\pi_1^*$  orbital are added as broken lines. The best fit ( $\varphi = 31.4^\circ$ ) is marked by the solid line.

As can be seen in Figure 5.5, the experimental points could be best-fitted with the theoretical curve corresponding to the tilt angle of  $\varphi = 31 \pm 5^\circ$  (the large error are mostly related to the uncertainty in the value of the twist angles  $\vartheta$ ) (Shaporenko et al. '03). This angle is slightly larger than the respective values for H-MBP SAMs on noble metal substrates ( $23^\circ$  for Au and  $18^\circ$  for Ag) (Frey et al. '01), but quite close to the corresponding angle for SAMs formed from 4-hydroxy-1,1'-biphenyl on hydrogenated Si (111) substrates ( $28.7^\circ$ ) (Zharnikov et al.). Note that the same assumptions concerning the 2D-arrangements of the biphenyl moieties have been made for H-MBP on Au and on Ar (Frey et al. '01), and 4-hydroxy-1,1'-biphenyl on hydrogenated Si (Zharnikov et al.), which allows the direct comparison of the derived tilt angles.

### 5.3.2 Chemical Composition

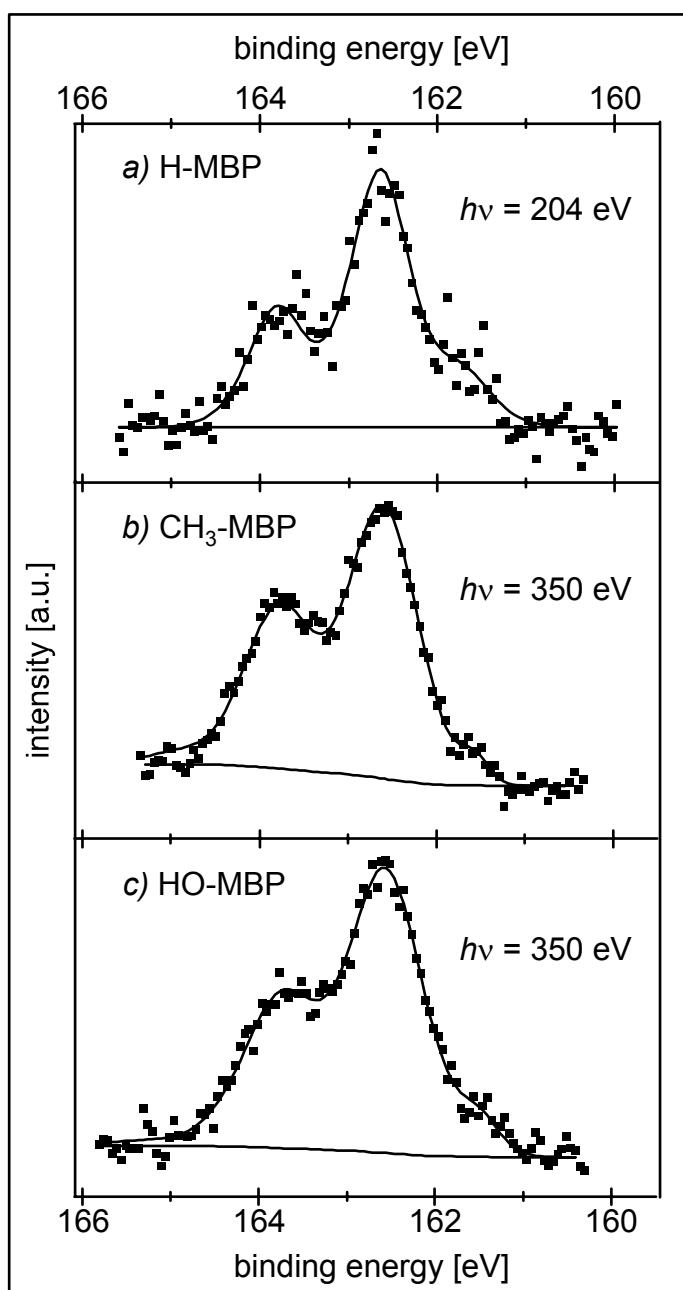
The chemical composition of the grafted 4'-substituted-4-mercaptobiphenyl (X-MBP) on the GaAs surface was studied by high resolution x-ray photoelectron spectroscopy (HRXPS).

Figure 5.6 shows the As 3d HRXPS spectra of (a) untreated (UT) and (b) freshly etched (FE) GaAs (Shaporenko et al. '03).



**Figure 5.6**

As 3d HRXPS spectra of (a) untreated (UT) and (b) freshly etched (FE) GaAs. The spectra are acquired at a photon energy of  $h\nu = 130$  eV. A decomposition of distinct spectral features by doublets related to individual chemical species is shown: light gray, GaAs; gray, elemental As ( $As^0$ ); The shoulders at the high binding energy side of the shadowed doublets correspond to As oxides ( $AsOx$ ).



**Figure 5.7**

*S 2p HRXPS spectra of GaAs coated with*  
a) 4-mercaptobiphenyl (H-MBP),  
b) 4'-methyl-4-mercaptobiphenyl (CH<sub>3</sub>-MBP) and  
c) 4'-hydroxy-4-mercaptobiphenyl (HO-MBP).

*Different photon energies  $h\nu$  were used. A dominant doublet at 162.6 eV (S 2p) suggests the presence of thiolate on the surface.*

The photon energy of  $h\nu = 130$  eV corresponds to a penetration depth of only 2 nm (Lindau & Spicer '74; Powell '74) allowing to evaluate the chemical composition of the

topmost layers. The spectra can be decomposed into the individual contributions related to stoichiometric GaAs (light gray, 41.1 eV), elemental arsenide ( $\text{As}^0$ , gray, 41.8 eV) and a broad peak at a high binding energy ( $\sim 44$  eV), which can be assigned to arsenide oxide ( $\text{AsOx}$ ). In the UT GaAs the arsenide oxide is quite dominant, but by the etching process it is drastically reduced to approximately 16 % (Shaporenko et al. '03).

The S  $2p$  core level spectra of GaAs coated with 4'-substituted-4-mercaptobiphenyl (X-MBP) measured at different photon energies  $h\nu$  are presented in *Figure 5.7* (Shaporenko et al. '03). A dominant S  $2p$  doublet at a binding energy of 162.6 eV (S  $2p$ ) is characteristic for thiolate species and verifies the covalent attachment of X-MBP onto GaAs (Heister et al. '01b; Himmelhaus et al. '98; Laibinis et al. '91; Zharnikov & Grunze '01). A minor contribution at 161.7 eV was also observed for GaAs with X-MBP monolayers and can be attributed either to atomic sulfur (S  $2p$ ) (Heister et al. '01b; Ishida et al. '99; Takiguchi et al. '00; Yang & Fan '02) or Ga  $3s$  emission (Moulder et al. '92).

*Figure 5.8* represents the As  $3d$  core level spectra of GaAs coated with (a) 4-mercaptobiphenyl (H-MBP) (Shaporenko et al. '03), (b) 4'-methyl-4-mercaptobiphenyl ( $\text{CH}_3$ -MBP) and (c) 4'-hydroxy-4-mercaptobiphenyl (HO-MBP), respectively. Again, due to the small photon energy ( $h\nu = 130$  eV) these spectra are mainly representative for GaAs surface. The spectra can be decomposed into individual contributions related to stoichiometric GaAs (light gray, 41.1 eV), elemental arsenide (gray, 41.8 eV,  $\text{As}^0$ ), and arsenide bound to sulfur (black, 42.4 eV,  $\text{AsS}$ ). The presence of the latter component also provides a clear evidence for the covalent attachment of X-MBPs to surface arsenides (Shaporenko et al. '03).

In addition to the above mentioned spectral components, there is a broad shoulder at a high binding energy ( $\sim 44$  eV) in *Figure 5.8*, which can be assigned to arsenide oxide ( $\text{AsOx}$ ). The respective extent of oxidation was comparable to that of a FE GaAs (*Fig. 5.6 b*, approx. 15-18 %), although the samples were kept for several days in ambient atmosphere after the grafting reaction. Thus, it can be concluded that all three X-MBPs protect the GaAs surface from further oxidation (Shaporenko et al. '03).

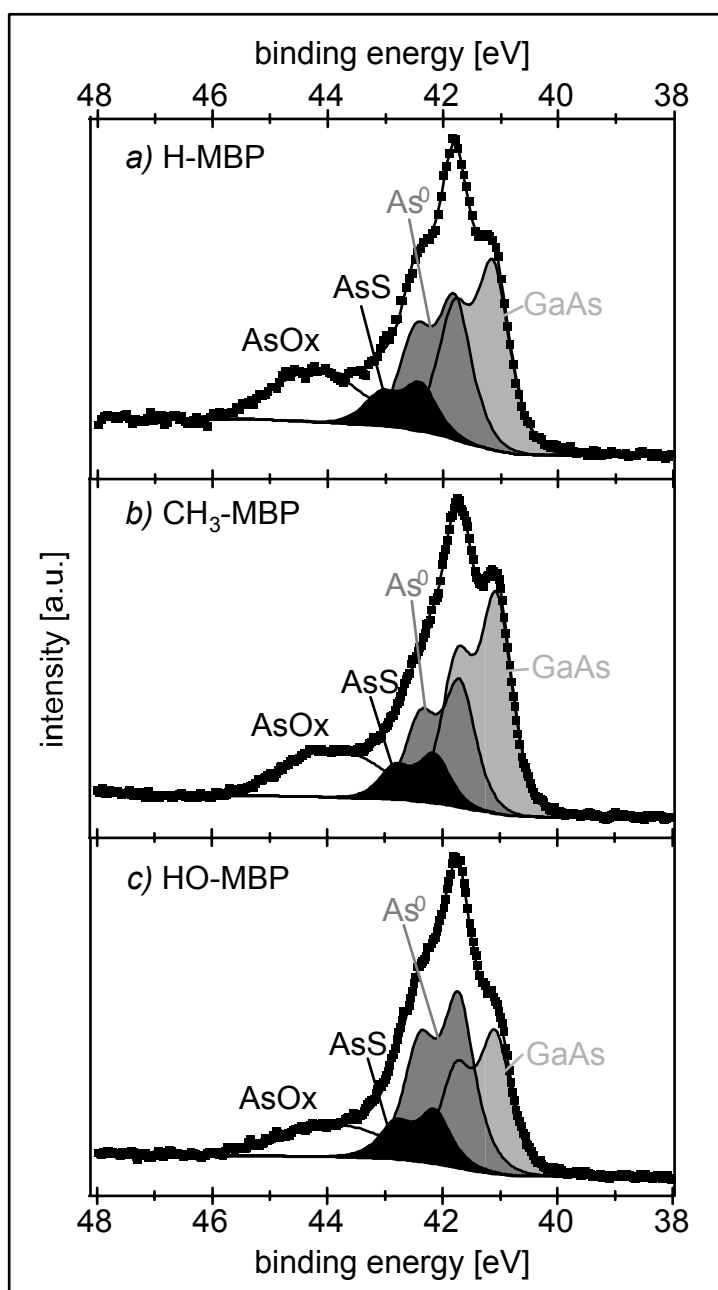


**Figure 5.8**

*As 3d HRXPS spectra of GaAs coated with (a) H-MBP, (b) CH<sub>3</sub>-MBP, and (c) HO-MBP. The Spectra are acquired at a photon energy of  $h\nu = 130$  eV. A decomposition of distinct spectral features by doublets related to individual chemical species is shown: light gray, GaAs; gray, elemental As, As<sup>0</sup>; black, As bound to sulfur, AsS. The shoulders at the high binding energy side of the shadowed doublets correspond to As oxides (AsOx). The appearance of the sulfur bonded As (black) confirmed the covalent attachment of X-MBP monolayers.*

## 6 Stability and Properties in Electrolyte

Systematic studies of the passivation of GaAs surfaces by self-assembled monolayers (SAMs) of 4'-substituted-4-mercaptobiphenyl (X-MBP) under physiological electrolyte are presented in the following.

Total surface free energies of etched and X-MBP covered GaAs surfaces and their dispersive and polar components were quantitatively estimated by contact angle measurements. Oxidation and reduction across the GaAs/4-mercaptobiphenyl (H-MBP) interface were measured by cyclic voltammetry. Electrochemical stability and properties of the GaAs/electrolyte and the three GaAs/4'-substituted-4-mercaptobiphenyl (X-MBP) monolayer/electrolyte interfaces were characterized by impedance spectroscopy.

### 6.1 Wetting and Surface Free Energy

From contact angle measurements the total surface free energy of the freshly etched (FE) and 4'-substituted-4-mercaptobiphenyl (X-MBP) coated GaAs surface and their dispersive and polar components were quantitatively estimated.

Sample	static water $\theta_{H_2O}$ [°]	advancing water $\theta_{adv}$ [°]	receding water $\theta_{rec}$ [°]	static diiodomethane $\theta_{dii}$ [°]	static glycerol $\theta_{gly}$ [°]
freshly etched	41	46	17	18	41
4-mercaptobiphenyl	77	85	62	34	70
4'-methyl- 4-mercaptobiphenyl	77	89	63	46	71
4'-hydroxy- 4-mercaptobiphenyl	60	64	42	26	43

**Table 6.1**

*Static, advancing and receding contact angle of water and static contact angle of diiodomethane and glycerol contact angles of the measured samples.*

In *Table 6.1* the static water contact angle of freshly etched (FE) GaAs is given,  $\theta_{H_2O}(FE) = 41^\circ$ . The advancing and receding contact angles were  $\theta_{adv}(FE) = 46^\circ$  and  $\theta_{rec}(FE) = 17^\circ$ , respectively. Such a high hysteresis  $\theta_{hys}(FE) = \theta_{adv}(FE) - \theta_{rec}(FE) = 29^\circ$  could be attributed to the surface heterogeneity (roughness) caused by etching as well as to the rapid oxidization of native (i.e. freshly etched) GaAs surface.

Deposition of 4-mercaptobiphenyl (H-MBP), 4'-methyl-4-mercaptobiphenyl (CH<sub>3</sub>-MBP) and 4'-hydroxy-4-mercaptobiphenyl (HO-MBP) resulted in the static water contact angles of  $\theta_{H_2O}(H-MBP) = 77^\circ$ ,  $\theta_{H_2O}(CH_3-MBP) = 77^\circ$  and  $\theta_{H_2O}(HO-MBP) = 60^\circ$ , respectively. The value obtained here is comparable to the corresponding values previously reported on Au [111] and Ag [111] grains, 70 ~ 85° (Kang et al. '98; Kang et al. '01; Tao et al. '97). Hysteresis for all measured substrates were comparable;  $\theta_{hys}(FE) = 29^\circ$ ,  $\theta_{hys}(H-MBP) = 23^\circ$ ,  $\theta_{hys}(CH_3-MBP) = 26^\circ$  and  $\theta_{hys}(HO-MBP) = 22^\circ$ . As observed by AFM, roughness rms values of the freshly etched and coated GaAs surfaces were comparable (*Chapter 5.1*). Thus, it is plausible that the observed hysteresis arises from the roughness of the substrates. In fact, similar hysteresis (~ 20°) was also found for the same monolayers on Au surfaces prepared by evaporation at room temperature (Kang et al. '01).

sample	total surface free energy $\gamma$ [mNm <sup>-1</sup> ]	dispersive component $\gamma_s$ [mNm <sup>-1</sup> ]	polar component $\gamma_p$ [mNm <sup>-1</sup> ]
freshly etched	54	27	27
4-mercaptobiphenyl	41	38	3
4'-methyl- 4-mercaptobiphenyl	35	30	5
4'-hydroxy- 4-mercaptobiphenyl	48	33	15

**Table 6.2**

*Total surface free energies,  $\gamma$ , dispersive components  $\gamma_s$ , and polar components  $\gamma_p$  of measured substrates.*

Table 6.2 gives the calculated surface free energies (Cap. 3.3.4) for the measured GaAs surfaces. Total surface free energies of GaAs coated with H-MBP and CH<sub>3</sub>-MBP were calculated to  $\gamma(H-MBP) = 41 \text{ mNm}^{-1}$  and  $\gamma(CH_3-MBP) = 35 \text{ mNm}^{-1}$ , respectively, indicating that the surfaces were rendered hydrophobic. The dispersive and polar components of the free energy could be obtained as  $\gamma_s(H-MBP) = 38 \text{ mNm}^{-1}$ ,  $\gamma_s(CH_3-MBP) = 30 \text{ mNm}^{-1}$ ,  $\gamma_p(H-MBP) = 3 \text{ mNm}^{-1}$  and  $\gamma_p(CH_3-MBP) = 5 \text{ mNm}^{-1}$ , respectively. Coating of GaAs with HO-MBP resulted in a more hydrophilic surface, whose total surface free energy was  $\gamma(HO-MBP) = 48 \text{ mNm}^{-1}$ . The dispersive and polar components of the engineered surface could also be calculated as  $\gamma_s(HO-MBP) = 33 \text{ mNm}^{-1}$  and  $\gamma_p(HO-MBP) = 15 \text{ mNm}^{-1}$ , respectively.

In comparison to the surface free energies of the same X-MBPs on Au surfaces,  $\gamma(H-MBP) = 50.5 \text{ mNm}^{-1}$ ,  $\gamma(CH_3-MBP) = 40 \text{ mNm}^{-1}$  and  $\gamma(HO-MBP) = 68 \text{ mNm}^{-1}$  (Kang et al. '98; Kang et al. '01), the total surface free energies obtained here are smaller. This can partially be explained by the different tilt angles that biphenyl backbones take with respect to the surface normal: e.g.  $\theta \sim 31^\circ$  on GaAs (Chapter 5.3.1) (Shaporenko et al. '03) and  $\theta < 20^\circ$  on Au for H-MBPs (Frey et al. '01; Kang et al. '01; Leung et al. '00). In fact, the lattice spacing of As on GaAs [100] surface (5.6 Å) is larger than that for Au on Au [111] ( $\sim 5.0 \text{ Å}$ ), suggesting the different grafting densities on these two surfaces. Even though the absolute values of free energies are different, the calculated dispersive and polar components on GaAs showed a good agreement with the previous results on Au (Kang et al. '98; Kang et al. '01), that is, the functional groups influence the polar components but not the dispersive components.

## 6.2 Electrochemical Processes across the Interface

Electrochemical processes across the GaAs/4-mercaptobiphenyl (H-MBP) interface were studied by cyclic voltammetry.

The first scan of cyclic voltammograms of freshly etched (FE, 1 min in HCl) GaAs is presented as a *broken line* in Figure 6.1, exhibiting a large oxidation at anodic potentials. In comparison to our previous results from the “photoetched” surface coated with amorphous arsenide layer (Adlkofer et al. '00), the maximum oxidation current of the bare GaAs was about 2 - 3 times larger. On the other hand, the reduction at the GaAs/electrolyte interface was smaller.

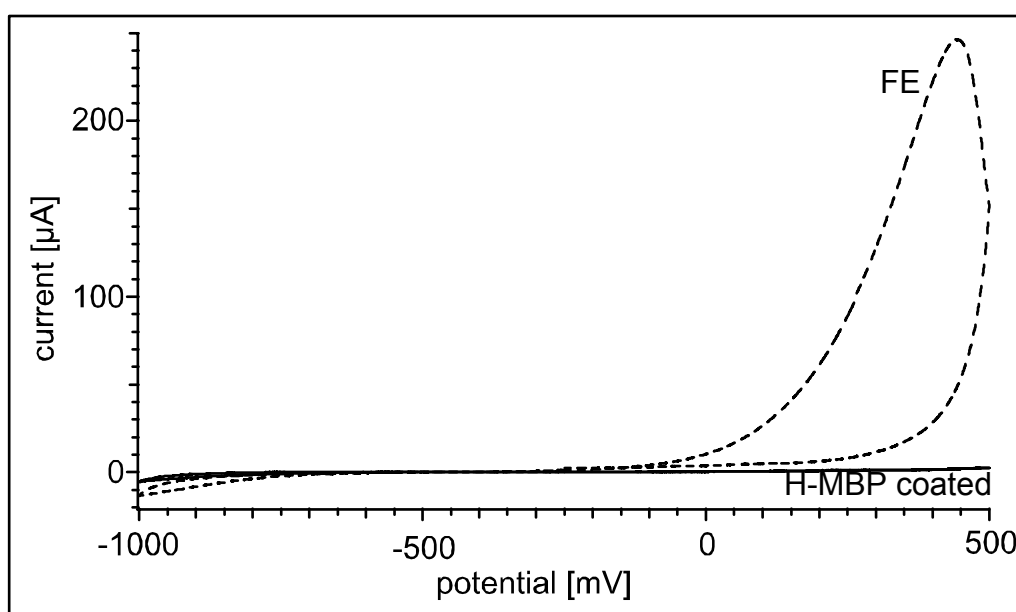


**Figure 6.1**

The first scan of cyclic voltammograms of (broken line) freshly etched (FE) GaAs and (solid line) 4-mercaptobiphenyl (H-MBP) coated GaAs. Each voltammogram was measured in 10 mM phosphate buffer with 10 mM NaCl (pH = 7.5) within the potential range between -1000 mV and +500 mV at a constant rate of  $25 \text{ mV s}^{-1}$ . Current across the interface was suppressed by deposition of 4-mercaptobiphenyl monolayers.

As the current across the interface was almost zero between -550 mV and -250 mV, a bias potential  $U_{bias} = -350 \text{ mV}$  for the following impedance spectroscopy experiments was chosen, which is not only close to the middle of this potential range but also almost at the same condition as in the previous studies (-360 mV) (Adlkofer

& Tanaka '01; Adlkofer et al. '00). Global shapes of the current-voltage scans were also different after each bias sweep, corresponding to the electrochemical instability of bare GaAs surfaces.

In contrast, current across the interface was dramatically suppressed by deposition of H-MBP monolayers (*Fig. 6.1, solid line*). Here, the H-MBP monolayer blocks the access of aqueous electrolytes to the GaAs electrode. Furthermore, it should be noted that the current signals after H-MBP coating was significantly smaller than those measured after octadecylthiol coatings (Adlkofer et al. '00), suggesting better insulating properties of H-MBP.

### 6.3 Stability and Interface Properties

Electrochemical stability and properties of the GaAs/electrolyte and the three GaAs/4'-substituted-4-mercaptobiphenyl (X-MBP) monolayer/electrolyte interfaces were characterized by impedance spectroscopy.

Figure 6.2 shows the impedance spectra, i.e. plots of absolute impedance and phase shift versus applied frequency, of bare GaAs ( $\blacktriangle$ ,  $\triangle$ ) shortly after etching and ( $\blacktriangledown$ ,  $\triangledown$ ) after 21 h. As the freshly etched (FE) GaAs were highly unstable, the first several spectra were measured in a smaller frequency range from 50 mHz to 50 kHz. Impedance spectra revealed a continuous and irreversible drift in 21 h.

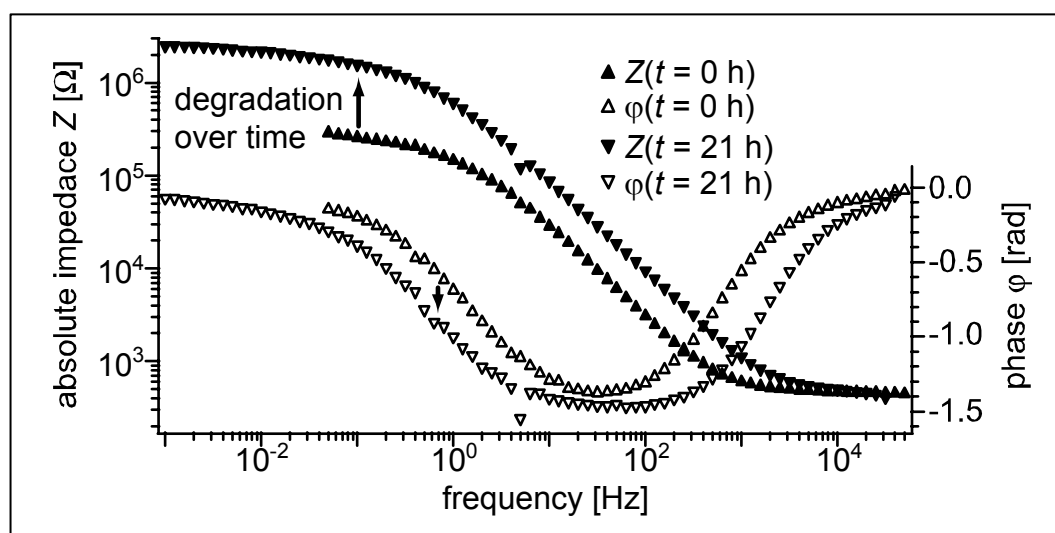


**Figure 6.2**

*Absolute impedance ( $\blacktriangle$ ) and phase shift ( $\triangle$ ) of bare GaAs shortly after etching and after 21 h ( $\blacktriangledown$ ,  $\triangledown$ ), plotted as a function of applied frequency. Due to rapid surface decomposition, the first several spectra were measured from 50 mHz to 50 kHz. In 10 mM phosphate buffer with 10 mM NaCl (pH = 7.5) the spectra revealed a continuous drift in 21 h.*

On the other hand, impedance spectra of 4-mercaptobiphenyl (H-MBP), 4'-methyl-4-mercaptobiphenyl (CH<sub>3</sub>-MBP), and 4'-hydroxy-4-mercaptobiphenyl (HO-MBP) coated GaAs were stable within the frequency range between 1 mHz and 50 kHz for more than 20 h (Fig. 6.3).

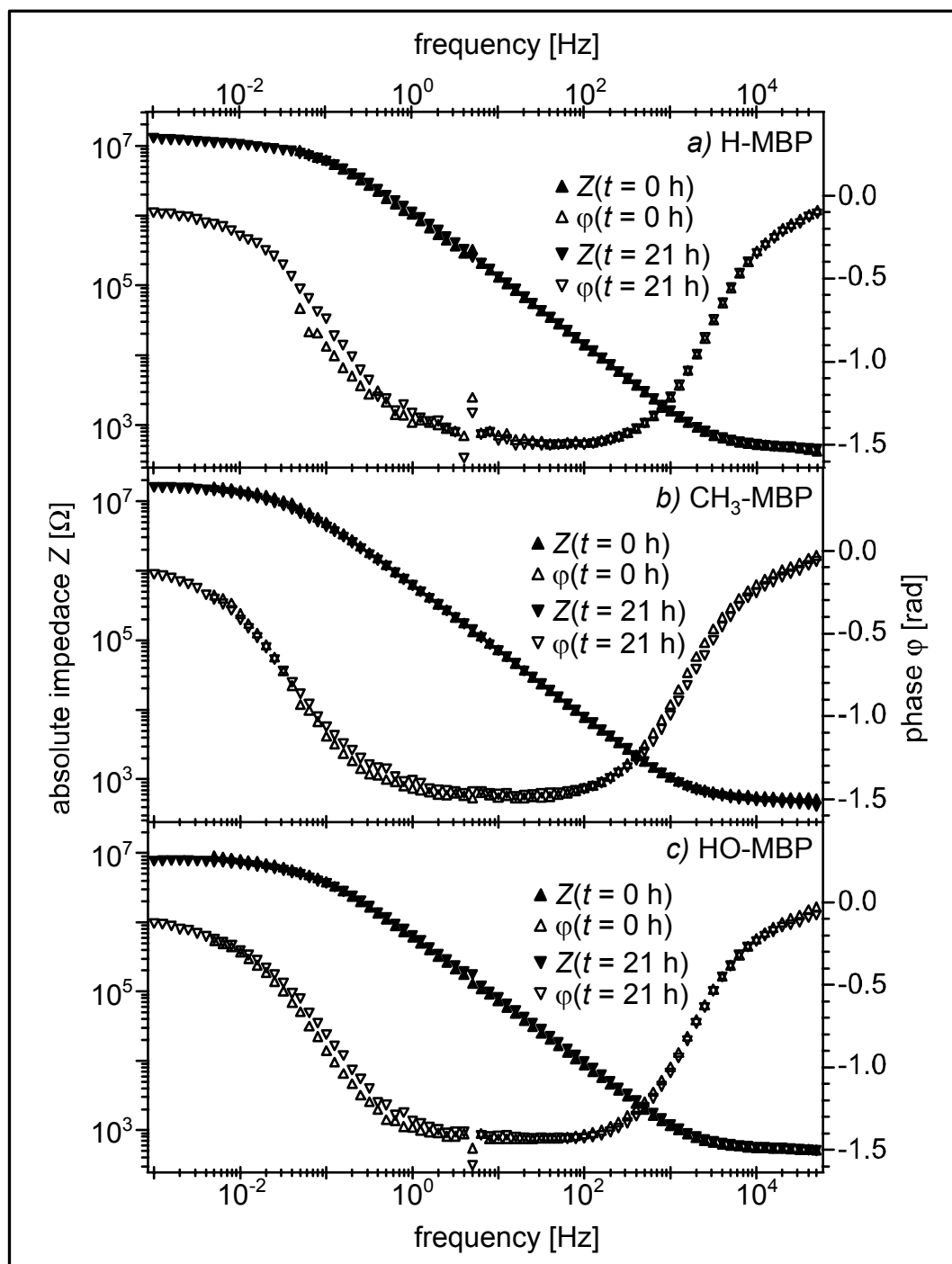


**Figure 6.3**

Impedance spectra of GaAs coated with (a) H-MBP, (b) CH<sub>3</sub>-MBP, and (c) HO-MBP. Absolute impedance ( $\blacktriangle$ ) and phase shift ( $\triangle$ ) of the first measurement and after measured for 21 h ( $\blacktriangledown$ ,  $\triangledown$ ) in 10 mM phosphate buffer with 10 mM NaCl (pH = 7.5), plotted as a function of applied frequency. Spectra were reproducible within a wide frequency range between 1 mHz and 50 kHz for more than 20 h.

Interface resistance  $R_p$ , and interface capacitance  $C$ , can be calculated from the measured spectra using the simplified equivalent circuit model (Fig. 3.11). Changes in the interface resistance and capacitance versus time were plotted for GaAs coated with ( $\square$ ) H-MBP, ( $\Delta$ )  $\text{CH}_3$ -MBP and ( $\circ$ ) HO-MBP in Figure 6.4 a and 6.4 b, respectively. For comparison, the corresponding results ( $\+$ ) for FE GaAs are also given in the Figure.

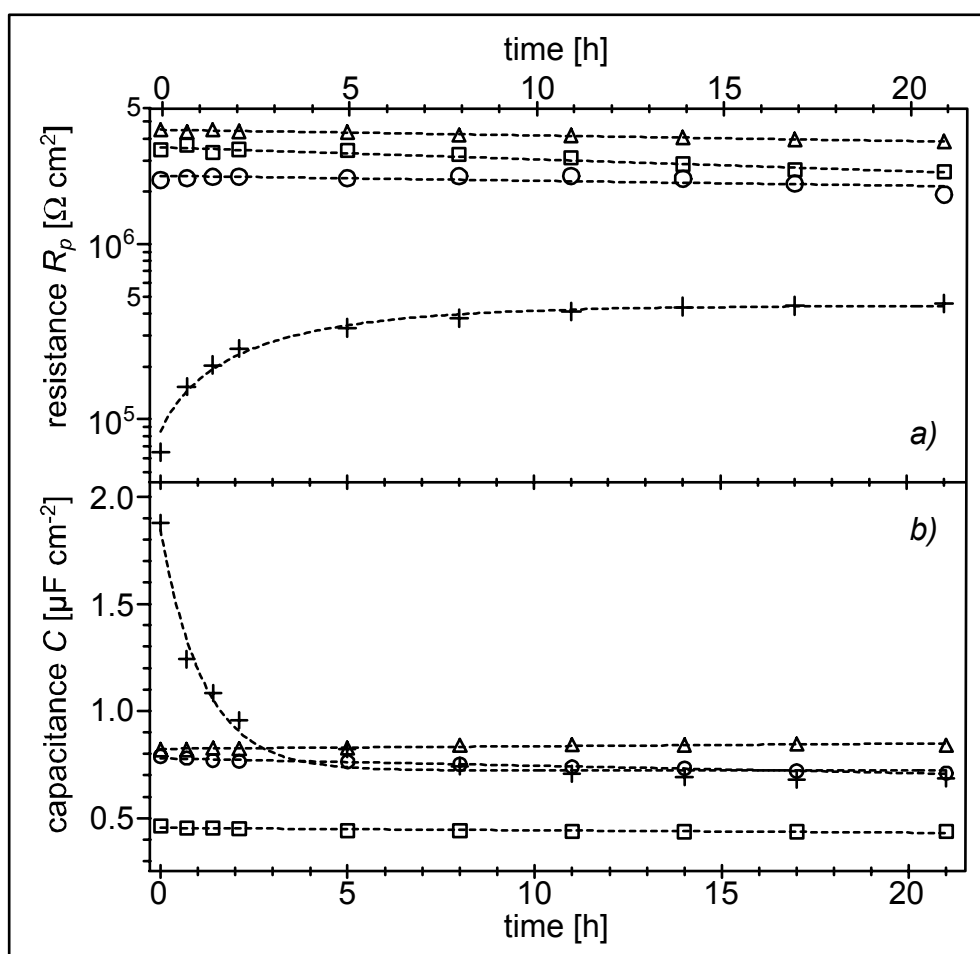


**Figure 6.4**

Changes in (a) interface resistance  $R_p$  and (b) interface capacitance  $C$  versus time for GaAs functionalized with ( $\square$ ) H-MBP, ( $\Delta$ )  $\text{CH}_3$ -MBP and ( $\circ$ ) HO-MBP. In contrast to FE GaAs ( $\+$ ), deposition of monolayers resulted in stabilization of GaAs/electrolyte interface for more than 20 h. The lines are given to guide the eye.

As can be seen, freshly etched GaAs exhibited a continuous increase in interface resistance from  $R_p(\text{FE}, t = 0 \text{ h}) = 64 \text{ k}\Omega \text{ cm}^{-2}$  (first measurement) to  $R_p(\text{FE}, t = 21 \text{ h}) =$

0.46 M $\Omega$  cm<sup>2</sup> at  $t = 21$  h. Interface capacitance also decreased continuously from  $C(FE, t = 0 h) = 1.9 \mu\text{F cm}^{-2}$  to  $C(FE, t = 21 h) = 0.69 \mu\text{F cm}^{-2}$ , reflecting the formation of an insoluble surface layer (Menezes & Miller '83). In contrast, GaAs functionalized with three types of 4'-substituted-4-mercaptobiphenyls (X-MBPs) showed stable interface resistances (within the fit error of 10 %) for more than 20 h,  $R_p(H-MBP) = 3.2 \text{ M}\Omega \text{ cm}^2$ ,  $R_p(CH_3-MBP) = 4.2 \text{ M}\Omega \text{ cm}^2$  and  $R_p(HO-MBP) = 2.3 \text{ M}\Omega \text{ cm}^2$ . The comparison of these values to that of FE GaAs,  $R_p(FE, t = 0 h) = 64 \text{ k}\Omega \text{ cm}^2$  implies that the deposition of a X-MBP monolayer caused a significant increase in interface resistance by a factor of  $50 \pm 15$ . Noteworthy, the interface resistance is highest for the most hydrophobic coating (*Chapter 6.1*) and lowest for the most hydrophilic one. As can be seen in *Figure 6.4 b*, the monolayer-coated GaAs also showed very stable interface capacitance (within the fit error of 10 %),  $C(H-MBP) = 0.45 \mu\text{F cm}^{-2}$ ,  $C(CH_3-MBP) = 0.83 \mu\text{F cm}^{-2}$  and  $C(HO-MBP) = 0.75 \mu\text{F cm}^{-2}$ . This coincides with the results from cyclic voltammetry experiments (*Chapter 6.2*), showing that the X-MBP monolayer blocks electrochemistry at the interface effectively.

The results obtained here also confirmed that all three of the functional X-MBP monolayers can realize effective passivation against electrochemical degradation in electrolytes. Furthermore, the aromatic backbones can be cross-linked with low energy electrons (Geyer et al. '99), which is promising to realize even more stable surface coating in aqueous electrolytes.

## 7 Functionalized GaAs-Based 2DEG Device

After the systematic studies of the X-MBP monolayers on bulk GaAs in air and under physiological electrolytes this system was transferred to a GaAs surface of a device with a two-dimensional electron gas (2DEG) near the surface ( $d = 60$  nm). The different dipole moments of the grafted 4-mercaptobiphenyl (H-MBP), 4'-hydroxy-4-mercaptobiphenyl (HO-MBP), and 4'-methyl-4-mercaptobiphenyl (CH<sub>3</sub>-MBP) molecules were detected by means of a change in the lateral resistance. The system showed sensitivity for the different dipole moments of the solvent molecules and appeared stable against organic solvents. Furthermore, the 2DEG resistance of the H-MBP coated sample was stable under physiological electrolyte for more than three hours. The processing and measurements were done at the Walter Schottky Institute, TU München in close cooperation with S. Luber (Luber et al. in print; Luber et al. '02). Moreover, the same strategy can directly be transferred onto various semiconductor heterostructures in the proximity of GaAs surfaces, such as near-surface quantum dots (QDs) (Adlkofer et al. '02; Duijs et al. '01), which might realize the design of sensors on electro-optical devices.

### 7.1 System and Device

#### 7.1.1 The Two-Dimensional Electron Gas System

The band structure of a GaAs/AlGaAs heterostructure is shown in *Figure 7.1*. A triangular potential well is formed at the inner interface between the AlGaAs and GaAs layer which, when filled with electrons, acts as a two-dimensional electron system. By doping the AlGaAs layer with an electron donor like silicon (Si), electrons diffuse to the considerably lower seated potential well and stay there confined in z-direction and freely moveable in the x-y plane. The z-confinement causes a energy quantization and thus the formation of subbands. At low temperatures, only the lowest subband is occupied and the system is called a "two-dimensional electron gas" (2DEG). At higher temperatures usually several subbands are partially filled and the correct denotation for the system is "quasi two-dimensional electron gas". In the rest of the present work this distinction will not be made. At higher temperatures the possibility that electrons are thermally excited to the potential well formed by the

dopant atoms must also be considered. This can complicate the situation as two conductive channels have to be taken into account at the same time, both featuring different electron mobilities.

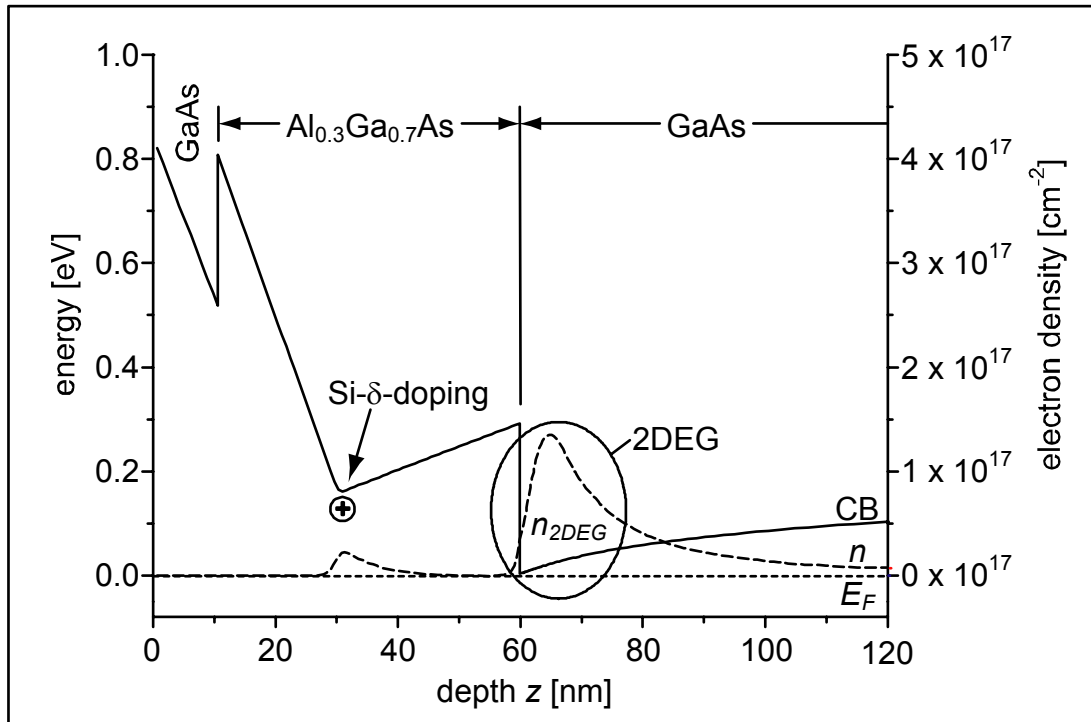


**Figure 7.1**

Calculated (nextnano<sup>3</sup>, Walter Schottky Institute, TU München) conduction band edge (CB, solid line) and electron density ( $n$ , broken line) of the 2DEG system near the surface ( $d = 60$  nm) at 295 K. The Si- $\delta$ -doping can be identified by the V-like notch in the conduction band at 30 nm depth. The Fermi energy level ( $E_F$ ) is given by the dashed line.

### 7.1.2 Device

GaAs/AlGaAs heterostructures containing a 2DEG 60 nm beneath the surface were grown by molecular beam epitaxy (MBE) and patterned into Hallbar-like mesa structures by standard lithographic techniques, wet chemical etching and annealing of NiGeAu Ohmic contacts (Fig. 7.2). As a reference, on some of the samples TiAu Schottky gates were deposited (Luber et al. in print; Luber et al. '02).

Lateral resistance measurements in ambient conditions (at square resistances of the order of a few k $\Omega$ ) were performed in a 4-terminal resistance setup, imposing a constant current of 1  $\mu$ A between source and drain and recording the resulting

potential drop between two probes. Measurements under wet conditions close to transistor channel pinch-off (high lateral resistance) were performed in a two-terminal setup by biasing source to drain with a constant DC potential of 100 mV and recording the resulting current (*Fig. 7.2*).

A specifically designed flow chamber restricted the exposure of liquids to the central part of the sample surface, where the metal contacts were located outside the chamber. The flow-chamber was connected to a peristaltic pump. Sample and fluid temperature were controlled by a thermostat to 23°C.

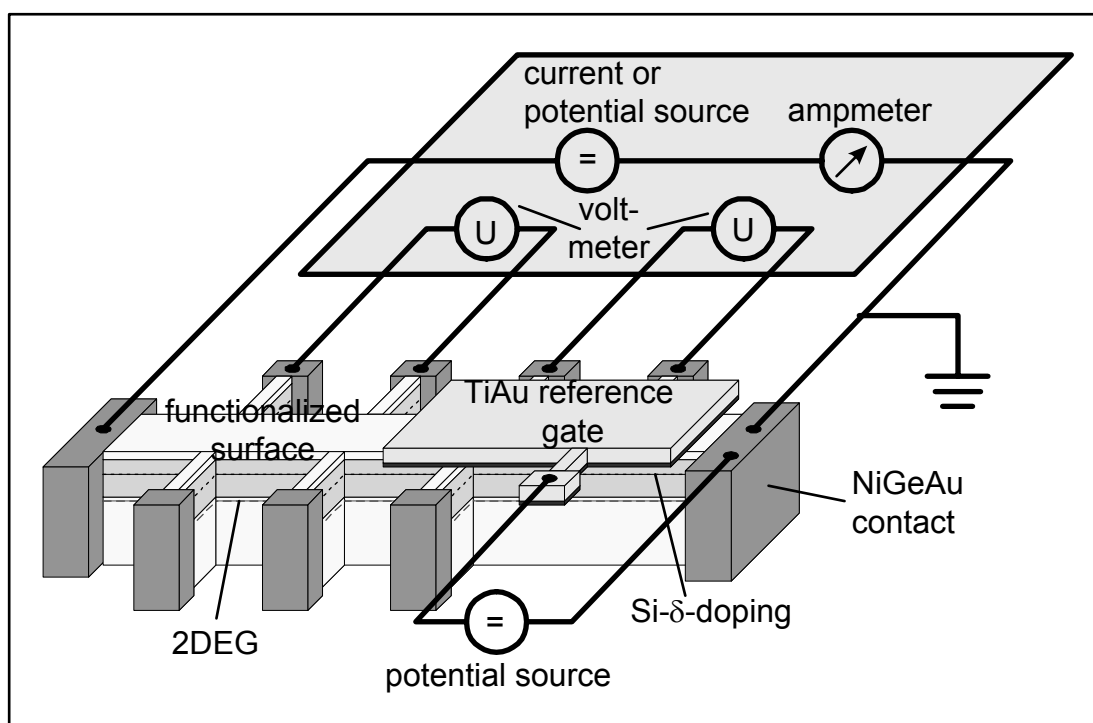


**Figure 7.2**

*Schematic view of the standard measurement setup for resistance measurements on the Hall-bar. Additional instruments like the thermostat are omitted for simplification. Lateral resistance measurements in ambient conditions were performed in a 4-terminal resistance setup, imposing a constant current of 1  $\mu$ A between source and drain and recording the resulting potential drop between two probes. Measurements under wet conditions close to transistor channel pinch-off were performed in a two-terminal setup by biasing source to drain with a constant DC potential of 100 mV and recording the resulting current.*

## 7.2 Dipole Moment of Grafted Molecules

As a first step the 4-terminal square resistances of the two-dimensional electron gas (2DEG) device coated with 4-mercaptobiphenyl (H-MBP), 4'-hydroxy-4-mercaptobiphenyl (HO-MBP), and 4'-methyl-4-mercaptobiphenyl (CH<sub>3</sub>-MBP) were measured in air (Luber et al. in print; Luber et al. '02).

Conjugation between 4'-substituents and thiolate can introduce different molecular dipole moments, but all 4'-substituted-4-mercaptobiphenyl (X-MBP) were covalently attached to the surface arsenide by the thiolate group (*Chapter 5.3.2*). The dipole moments along the molecular axis and electronic densities of the H-MBP, HO-MBP and CH<sub>3</sub>-MBP molecules were estimated from density-functional-theory calculations (CACHÉ® software using the DZVP basic-set at the GGA-B88LYP level) (*Table 7.1*).

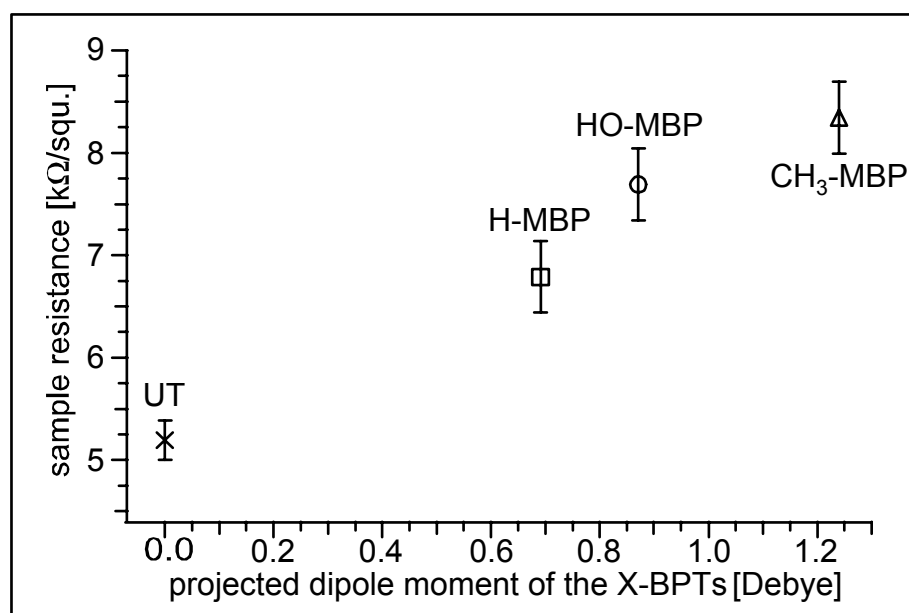


**Figure 7.3**

Square resistance of the coated 2DEG device as a function of the projected dipole moment along the molecular axis of the 4-mercaptobiphenyl (H-MBP), 4'-hydroxy-mercaptobiphenyl (HO-MBP), and 4'-methyl-4-mercaptobiphenyl (CH<sub>3</sub>-MBP) molecules. As a reference the square resistance of the untreated (UT) sample is shown (Luber et al. in print; Luber et al. '02).

In *Figure 7.3* the measured square resistances are plotted as a function of the projection of the individual dipole moments along the molecule's long axis. As a reference the square resistance of the untreated (UT) sample is shown. The grafting

of molecules with different dipole moment shows a clear influence on the sheet resistance of the surface-near 2DEG (Luber et al. in print; Luber et al. '02).

The surface functionalized GaAs/AlGaAs heterostructure device is operated as a field effect transistor (FET) whose carrier concentration in the 2D sheet is controlled by the surface potential via the band bending; hence, any change in measured sheet resistance can be directly correlated to a change in surface potential. The adsorption of a dipole layer results in a change of the electron work function, i.e. the energy needed to lift an electron from the Fermi level  $E_F$  to the vacuum level (conduction band edge  $E_{CB}$ ). The work function is given by the sum of electron affinity ( $\Delta\chi$ ) and surface band bending ( $\Delta V_{bb}$ ),  $\Delta\Phi = \Delta\chi + \Delta V_{bb} + E_{CB} - E_F$ . Here, the variation of electron affinity due to dipole adsorption is given by the potential drop through the layer of adsorbed molecules. In the simplest approximation, this oppositely charged double layer can be described by an ideal parallel plate capacitor, as far as the dipole "length"  $w$  (distance between the centers of the distribution of opposite charge  $q$ ) exceeds the lateral dipole spacing  $a$  and is much smaller than the overall lateral extension of the monolayer. By elementary electrostatics one obtains for the potential drop (Helmholtz equation)

$$\Delta V_{dip} = np \cos\Theta / \epsilon \epsilon_0, \quad (7.1)$$

where  $n$  is the area-density of dipoles,  $p = qw$  their absolute dipole moment,  $\Theta$  is the dipole vector's tilting angle with respect to the surface normal and  $\epsilon$  the layer's dielectric constant (*Fig. 3.2*). In general,  $\epsilon$  cannot be identified with the bulk macroscopic value, but rather it takes into account the mutual polarizability of the molecules in the monolayer (Lüth '97). A similar consideration holds for the molecular dipole moment: In a closely packed layer it differs considerably from the value of free molecule due to electronic charge redistribution (Taylor & Bayes '94; Vager & Naaman '02). Nevertheless, a linear dependence of electron affinity  $\Delta\chi$  from absolute dipole moment  $p$  (free molecule value) as in *Equation 7.1* has been observed for benzoic acid adsorption on GaAs (Bastide et al. '97).

However, a change of the band bending due to dipole adsorption is less evident, as such an ideal parallel plate capacitor has no external electrical field. In fact, the X-MBP monolayer might not be treated as an ideal capacitor due to several reasons:

First, the assumption  $w \gg a$  is not fulfilled, taking the measured X-MBP layer thickness  $d = 10 \pm 2 \text{ \AA}$  (Chapter 5.2) as an estimate for  $w$  and  $a = 5.6 \text{ \AA}$  from a mean X-MBP density of  $n = 0.031 \text{ \AA}^{-2}$  (Bain '92). Second, formation of the chemical bond would modify the surface state density and energy distribution (Adlkofer et al. '02; Duijs et al. '01). Such a change of the surface state density shifts the position of the Fermi level (hence the band bending) which for GaAs is pinned at mid-gap, approximately. However, this contribution should not distinguish between the three X-MBPs since substituting the endgroup produces only minor changes in the electron density of the binding thiol (S-H) group. Additional deviations can be due to local defects at the edges of the Hallbar (Fig. 7.2) where the electrical field may leak outside.

molecule	projected dipole moment $ \mu_{proj} $ [Debye]	calculated potential drop $\Delta V_{dip}$ [mV]	gate potential $\Delta V_{gate}$ [mV]
4-mercaptobiphenyl	0.691	160	90
4'-hydroxy-4-mercaptobiphenyl	0.871	200	120
4'-methyl-4-mercaptobiphenyl	1.240	280	140

**Table 7.1**

*Calculated projection of the dipole moments along the molecule's long axis of 4-mercaptobiphenyl (H-MBP), 4'-hydroxy-4-mercaptobiphenyl (HO-MBP) and 4'-methyl-4-mercaptobiphenyl (CH<sub>3</sub>-MBP) (CACHe® software using the DZVP basic-set at the GGA-B88LYP level). Calculated potential drop across the 4'-substituted-4-mercaptobiphenyl (X-MBP) monolayers and gate potential which was applied to reach the same relative resistance changes as the X-MBP coated 2DEG devices (Luber et al. in print; Luber et al. '02).*

Furthermore, only a fixed and constant electrostatic potential on top of the monolayer, e.g. in an electrolyte at a reference potential, will induce the full bend bending by the potential drop through the dipole monolayer. Under this conditions the potential drop through the dipole layer  $\Delta V_{dip}$  would result in a shift of the surface potential and alter the band bending (Chai & Cahen '02; Wu et al. '01). Because of

the limits of the experimental setup there is air or an insulating dielectric liquid on top of the monolayer and the electrostatic boundary condition is not well defined.

Nevertheless, by estimating the order of magnitude of such potential drops and comparing them to reference measurements where the surface potential is directly controlled by a metal gate, a correlation between  $\Delta V_{dip}$  and  $\Delta V_{bb}$  was found. The potential drop across the H-MBP, HO-MBP and CH<sub>3</sub>-MBP monolayers (*Fig. 7.3*) were estimated (*Eq. 7.1*) to  $\Delta V_{dip}(H-MBP) = 160$  mV,  $\Delta V_{dip}(HO-MBP) = 200$  mV and  $\Delta V_{dip}(CH_3-MBP) = 280$  mV, respectively, by assuming  $n = 0.031 \text{ \AA}^{-2}$  (Bain '92),  $\epsilon = 4.5$  (Sabatani et al. '93) and a mean  $\Theta = 30^\circ$  (*Chapter 5.3.1*), the results are given in *Table 7.1*. The order of magnitude of the resistance changes fits remarkably well to independent reference measurements: A standard metal Schottky gate yielded the same relative resistance changes as observed for the H-MBP, HO-MBP and CH<sub>3</sub>-MBP monolayers at the gate potentials of  $\Delta V_{gate} = 90$  mV, 120 mV and 140 mV, respectively, also given in *Table 7.1*.

Operating the 2DEG device as a field-effect-transistor (FET) enables to measure even the small deviations in the dipole moments of the grafted X-MBPs terminated with X = H, hydroxyl (X = OH) and methyl (X = CH<sub>3</sub>).

### 7.3 Stability and Sensitivity against Polar Solvents

As the next step, the two-terminal resistance (*Fig. 7.2*) of a two-dimensional electron gas (2DEG) device coated with 4'-substituted-4-mercaptobiphenyl (X-MBP) was measured in presence of a variety of organic solvents in order to measure the stability and sensitivity of the device (Luber et al. in print; Luber et al. '02).

After the injection of the solvent the resistance quickly increased from about 70 k $\Omega$  to above 10 M $\Omega$ , almost fully depleting the conductive layer of the field effect transistor (FET). After about 10 min the system reached the saturation value dependent of the solvent (*Fig. 7.4*). After each solvent the sample was purged by N<sub>2</sub> and recovered the ambient value (70 k $\Omega$ ) within the same order of magnitude confirming the stability of the coated device against organic solvents. Noticeable, a *non-polar* solvent octane did not induce any resistance change. In contrast to the *coated* 2DEG devices, the samples with a *bare* GaAs surface showed much less reproducible and unstable results.

solvent	Molecular dipole moment $p$ [Debye]	Bulk dielectric constant $\epsilon$
octane	0	1.95
methanol	1.7	32.8
ethanol	1.68	24.3
isopropanol	1.66	18.8
acetonitril	3.92	36.9
pentanol	1.65	14.3
acetone	2.88	20.6

**Table 7.2**

*Molecular dipole moment  $p$  and the bulk dielectric constant  $\epsilon$  of the measured solvents taken from the Beilstein data base.*

These results not only prove the stability of the X-MBP coated 2DEG devices against organic solvents, but it can also be used as a chemical sensing device for polar solvents, where the resistance change is related to the molecular dielectric properties of the solvents. A similar sensitivity to polar organic solvents has been reported on

GaN devices (Neuberger et al. '01).

The semiconductor/X-MBP monolayer/solvent system was empirically analyzed like the system without solvent in *Chapter 7.2*, correlating the resistance changes with the dielectric properties of the liquids. *Table 7.2* shows the molecular dipole moment  $p$  and the bulk dielectric constant  $\epsilon$  of the measured solvents taken from the *Beilstein* data base.

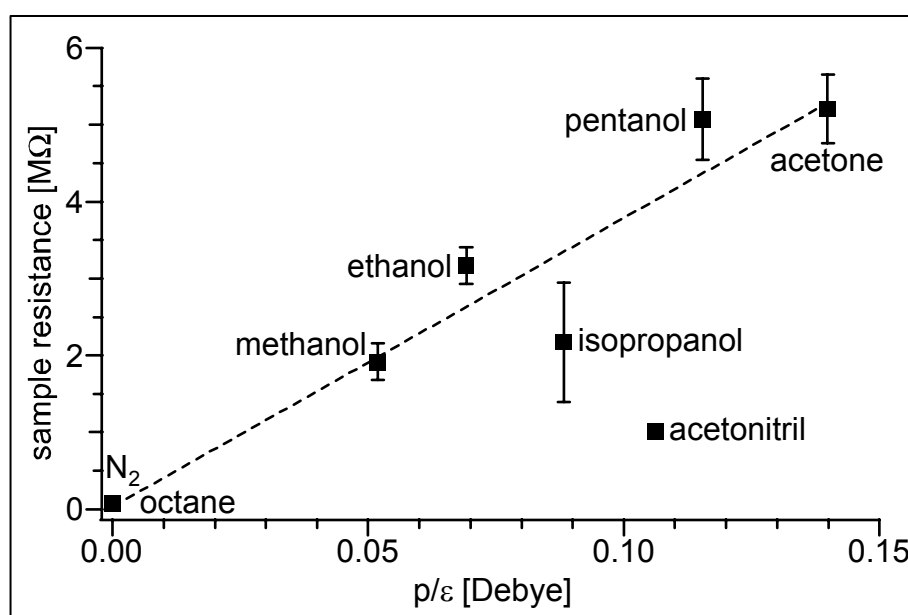


**Figure 7.4**

Saturation resistances of the 4'-substituted-4-mercaptobiphenyl (X-MBP) coated 2DEG devices as a function of  $p / \epsilon$  of the solvents (*Table 7.2*). The line is given to guide the eye (Luber et al. in print; Luber et al. '02).

*Figure 7.4* displays the saturation resistances plotted as a function of molecular dipole moment  $p / \epsilon$  normalized to the bulk dielectric constant for each solvent. The measured saturation resistance increased linearly with  $p / \epsilon$ , acetonitrile and isopropanol were the only exceptions. Potentials lower than -200 mV had to be applied to obtain two-terminal resistances in the same range on the reference sample with the standard metal Schottky gate. Noticeable, the resulted surface potentials correspond to the sum of the voltage drop  $V_{dip}$  of the X-MBP monolayer and the voltage drop across a first layer of adsorbed solvent molecules estimated according to *Equation 7.1*. This suggested the monomolecular adsorption of solvent molecules

(“bimolecular” monolayer) (Chai & Cahen '02; Hutchison et al. '01), whose dipole moments are aligned parallel to that of the X-MBP molecules. In spite of the unknown orientation of solvent molecules on X-MBP monolayer surfaces, this crude approximation seems to agree with the obtained resistance.

The X-MBP coated 2DEG device showed sensitivity for the different dipole moments of the solvent molecules and appeared stable against organic solvents.

## 7.4 Stability in Aqueous Electrolyte

Figure 7.5 shows the resistance of a 4-mercaptobiphenyl (H-MBP) coated 2DEG device under physiological conditions (in aqueous electrolyte, pH = 6.5) as a function of time. As a reference the resistance of an untreated (UT) sample is given (Luber et al. in print; Luber et al. '02). The H-MBPs of this monolayer were cross-linked by low energy e-beam-irradiation before measurement (Geyer et al. '99).

As expected, the bare reference sample rapidly degrades due to successive surface decomposition, whereas the H-MBP passivated sample showed good stability over several hours. The observed slight resistance increase can be attributed to defects in the H-MBP layer. Such defects are likely to occur for the considerably large active area of the device ( $\sim 3 \text{ mm}^2$ ), at least at its mesa edges (Fig. 7.1.2), and can be effectively reduced by miniaturization and planarization / encapsulation.

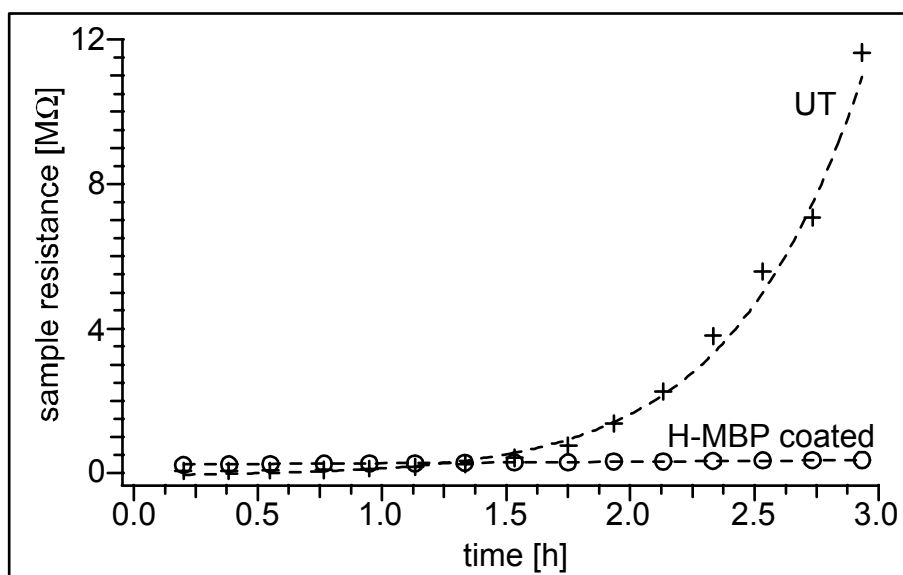


**Figure 7.5**

Resistance of a 4-mercaptobiphenyl (H-MBP) coated 2DEG device under physiological as a function of time. As a reference the resistance of an untreated (UT) sample is given (Luber et al. in print; Luber et al. '02).

## 8 Conclusions

This study demonstrated the stable and functional engineering of stoichiometric GaAs [100] surfaces by depositing a new class of organic self-assembled monolayers (SAMs) composed of 4-mercaptobiphenyl derivatives (X-MBPs).

As presented in *Chapter 4*, the conditions of the grafting reaction were firstly optimized by changing two parameters: solvent polarity and reaction temperature. Qualities of the resulting SAMs were evaluated by ellipsometry (film thickness) and AC impedance spectroscopy (electric resistance). Among three different solvents (dimethylformamid, toluene, ethanol), the grafting reaction in ethanol resulted in the best quality for the SAMs of 4-mercaptobiphenyl (H-MBP). When the monolayers were prepared at three different temperatures (20, 35, and 50 °C), the optimal grafting could be achieved at 50 °C.

*Chapter 5* deals with the full characterizations of the optimized SAMs and the bare GaAs (prepared by wet chemical etching) in dry states, i.e. either in ambient or in vacuum, using various surface sensitive techniques. Surface topographies of the SAMs and that of the bare GaAs were measured by atomic force microscopy (AFM), implying that the deposition of the monolayer did not cause any surface roughening (rms < 3.5 Å). Thicknesses of the SAMs were estimated to be  $10 \pm 2$  Å by ellipsometry, which suggests that the X-MBP molecules take almost an upright orientation. The angular dependence of the  $\pi_1^*$  resonance intensity obtained from near edge x-ray adsorption fine structure (NEXAFS) spectroscopy implied that MBP backbones are highly ordered, whose tilt angle to the surface normal is  $31 \pm 5^\circ$ . Surface chemical compositions before and after the monolayer deposition were studied by high resolution x-ray photoelectron spectroscopy (HRXPS). The covalent binding of sulfur and arsenide could be detected from As 3d spectra, while S 2p spectra indicate the presence of thiolate on GaAs. Furthermore, the intensities of arsenide oxide peaks in As 3d spectra measured for the engineered GaAs remained constant after several days in ambient, implying the high chemical stability of the monolayer-coated GaAs against the oxidation in air.

In *Chapter 6*, the functionalized GaAs surfaces were characterized in contact with water. Firstly, the total surface free energy and its polar and dispersive components were calculated from the contact angle measurements (water, diiodomethane, and glycerol) for each X-MBP monolayer, showing a strong dependence of the dispersive component on 4'-substitutions. In fact, such wetting characteristics obtained here provide quantitative measures for the surface compatibilities to lipid membranes and biopolymers. Cyclic voltammetry exhibited that deposition of 4-mercaptobiphenyl (H-MBP) monolayer resulted in a clear suppression of electrochemistry at pH = 7.5. Indeed, impedance spectra measured at a cathodic potential of -350 mV demonstrated that the interface resistance was significantly increased by a factor of  $50 \pm 15$  by the coating with X-MBPs. Furthermore, both interface resistance and capacitance of the coated GaAs electrodes were stable for more than 20 h within the wide frequency range of 1 mHz to 50 kHz.

Based on the full characterizations for bulk GaAs mentioned above, a Hall-bar device with two-dimensional electron gas (2DEG) near the surface ( $d = 60$  nm) was functionalized with three different X-MBPs (X- = H-, HO-, and CH<sub>3</sub>-) according to the same protocol. The sheet resistance of 2DEG layer was clearly dependent on the dipole moments from the 4'-substituents (X- groups). The functionalized 2DEG device showed stable sheet resistances in the presence of aqueous electrolytes and different organic solvents without any pronounced degradation. Furthermore, the sheet resistance of the monolayer-coated device also seemed to be sensitive to the solvent polarities. The obtained results thus strongly suggest that the 2DEG devices coated with X-MBPs can be operated in various liquid environments, and are highly sensitive to the surface dipole moments.

Thus, the surface engineering method established in this study can provide stable and functional platforms with well defined surface characteristics, which can be utilized for the design of novel bio-inspired semiconductor devices by deposition of biopolymers and model cell membranes.

## Literature

Adlkofer, K., E. F. Duijs, F. Findeis, M. Bichler, A. Zrenner, E. Sackmann, G. Abstreiter, and M. Tanaka (2002).

“Enhancement of photoluminescence from near-surface quantum dots by suppression of surface state density.”

Phys. Chem. Chem. Phys. **4**: 785-790.

Adlkofer, K., and M. Tanaka (2001).

“Stable Surface Coating of Gallium Arsenide with Octadecylthiol Monolayers.”

Langmuir **17**(14): 4267-4273.

Adlkofer, K., M. Tanaka, H. Hillebrandt, G. Wiegand, E. Sackmann, T. Bolom, R. Deutschmann, and G. Abstreiter (2000).

“Electrochemical passivation of gallium arsenide surface with organic self-assembled monolayers in aqueous electrolytes.”

Appl. Phys. Lett. **76**(22): 3313-3315.

Agren, H., O. Vahtras, and V. Carravetta (1995).

“Near-edge core photoabsorption in polyacenes: model molecules for graphite.”

Chem. Phys. **196**: 47-58.

Allongue, P., and H. Catchet (1985).

“Band-Edge Shift and Surface Charges at Illuminated n-GaAs/Aqueous Electrolyte Junctions.”

J. Electrochem. Soc. **132**(1): 45-52.

Asai, K., T. Miyashita, K. Ishigure, and S. Fukatsu (1993).

“An application of electrolytic deposition for the electronic passivation of GaAs surfaces through the formation of thin organic films.”

Surf. Sci. **306**: 37-41.

Bain, C. D. (1992).

“A New Class of Self-Assembled Monolayers: Organic Thiols on Gallium Arsenide.”

Adv. Mater. **4**(9): 591-594.

Band, I. M., Y. I. Kharitonov, and M. B. Trzhaskovskaya (1979).

At. Data Nucl. Data Tables **23**: 443.

Bard, A. J., and L. R. Faulkner (1980).

“Electrochemical methods”

New York, Wiley Interscience.

Bastide, S., R. Butruillee, D. Cahen, A. Dutta, J. Libman, A. Shanzer, L. Sun, and A. Vilan (1997).

“Controlling the Work Function of GaAs by Chemisorption of Benzoic Acid Derivatives.”

J. Phys. Chem. B **101**(14): 2678-2684.

Batson, P. E. (1993).

“Carbon 1s near-edge-adsorption fine structure in graphite.”

Phys. Rev. B **48**: 2608-2610.

Bergveld, P. (1996).

“The future of biosensors.”

Sensors and Actuators A **56**: 65-73.

Bergveld, P. (2003).

“Thirty years of ISFETOLOGY

What happened in the past 30 years and what may happen in the next 30 years.”

Sensors and Actuators B **88**(1): 1-20.

Chai, L., and D. Cahen (2002).

“Electric signal transfer through nm-thick molecular bilayers.”

Mat. Sci. Engineering **19**(1-2): 339-343.

Chang, S., I. M. Vitomirov, L. J. Brillson, D. F. Rioux, P. D. Kirchner, G. D. Pettit, and J. M. Woodall (1991).

“Increased range of Fermi-level stabilization energy at metal/melt-grown GaAs(100) interfaces.”

J. Vac. Sci. Technol. B **9**: 2129-2134.

Chang, S.-C., I. Chao, and Y.-T. Tao (1994).

“Structures of Self-Assembled Monolayers of Aromatic-Derivatized Thiols on Evaporated Gold and Silver Surfaces: Implication on Packing Mechanism.”

J. Am. Chem. Soc. **116**(15): 6792-6805.

Cruickshank, D. W. J. (1956).

“A detailed refinement of the crystal and molecular structure of anthracene.”

Acta Crystallogr. **9**: 915.

Cui, Y., Q. Wei, H. Park, and C. M. Lieber (2001).

“Nanowire Nanosensors for Highly Sensitive and Selective Detection of Biological and Chemical Species.”

Science **293**: 1289-1292.

Dharani, A.-A., W. Zehner, R. P. Hsung, P. Guyot-Sionnest, and L. Sita (1996).

“Self-Assembly of Conjugated Molecular Rods: A High-Resolution STM Study.”

J. Am. Chem. Soc. **118**(13): 3319-3320.

Duijs, E. F., F. Findeis, R. A. Deutschmann, M. Bichler, A. Zrenner, G. Abstreiter, K. Adlkofer, M. Tanaka, and E. Sackmann (2001).

"Influence of Thiol Coupling on Photoluminescence of Near Surface InAs Quantum Dots."

Phys. Status Solidi B **3**: 871-875.

Frey, S., K. Heister, M. Zharnikov, M. Grunze, K. Tamada, R. J. Colorado, M. Graupe, O. E. Shmakova, and T. R. Lee (2000).

Isr. J. Chem. **40**: 81.

Frey, S., V. Stadler, K. Heister, W. Eck, M. Zharnikov, M. Grunze, B. Zeysing, and A. Terfort (2001).

"Structure of Thioaromatic Self-Assembled Monolayers on Gold and Silver."

Langmuir **17**: 2408-2415.

Fuxen, C., W. Azzam, R. Arnold, G. Witte, A. Terfort, and C. Wöll (2001).

"Structural Characterization of Organothiolate Adlayers on Gold: The Case of Rigid, Aromatic Backbones."

Langmuir **17**(12): 3689-3695.

Geyer, W., V. Stadler, M. Zharnikov, A. Götzhäuser, and M. Grunze (1999).

"Electron-induced crosslinking of aromatic self-assembled monolayers: Negative resists for nanolithography."

Appl. Phys. Lett. **75**(16): 2401-2403.

Goldberg, S. M., C. S. Fadley, and S. Kono (1981).

"Photoionization cross-sections for atomic orbitals with random and fixed spatial orientation."

Electron Spectrosc. Relat. Phenom. **21**(4): 285-363.

Heister, K., H.-T. Rong, M. Buck, M. Zharnikov, M. Grunze, and L. S. O. Johansson (2001a).

"Odd-Even Effects at the S-Metal Interface and in the Aromatic Matrix of Biphenyl-Substituted Alkanethiol Self-Assembled Monolayers."

J. Phys. Chem. B **105**(29): 6888-6894.

Heister, K., M. Zharnikov, M. Grunze, and L. S. O. Johansson (2001b).

"Adsorption of Alkanethiols and Biphenylthiols on Au and Ag Substrates: A High-Resolution X-ray Photoelectron Spectroscopy Study."

J. Phys. Chem. B **105**: 4058-4061.

Hellwege, K.-H., Ed. (1983).

"Landolt-Börnstein

Numerical Data and Functional Relationships in Science and Technologie

Group III: Crystal and Solid State Physics"

"Semiconductors

Physics of Non-Tetrahedrally Bounded Elements and Binary Compounds I"

Berlin, Springer-Verlag.

Hens, Z., and W. P. Gomes (1999).

"The Electrochemical Impedance of One-Equivalent Electrode Processes at Dark Semiconductor/Redox Electrodes Involving Charge Transfer through Surface States. 2. The n-GaAs/Fe<sup>3+</sup> System as an Experimental Example."

J. Phys. Chem. B **103**: 130-138.

Himmel, H.-J., A. Terfort, and C. Wöll (1998).

"Fabrication of a Carboxyl-Terminated Organic Surface with Self-Assembly of Functionalized Terphenylthiols: The Importance of Hydrogen Bond Formation."

J. Am. Chem. Soc. **120**: 12069-12074.

Himmelhaus, M., I. Gauss, M. Buck, F. Eisert, C. Wöll, and M. Grunze (1998).

"Adsorption of docosanethiol from solution on polycrystalline silver surfaces: an XPS and NEXAFS study."

J. El. Spectr. Rel. Phenom. **92**: 139.

Horowitz, G., P. Allongue, and H. Catchet (1984).

"Quantitative Comparison of Fermi Level Pinning at GaAs/Metal and GaAs/Liquid Junctions."

J. Electrochem. Soc. **131**(11): 2563-2569.

Horsley, J., J. Stöhr, A. P. Hitchcock, D. C. Newbury, A. L. Johnson, and F. Sette (1985).

"Resonance in the *K* shell excitation spectra of benzen and pyridine: Gas phase, solid, and chemisorbed states."

J. Chem. Phys. **83**(12): 6099-6107.

Hutchison, G. R., M.-A. Ratner, and T. J. Marks (2001).

"Adsorption of Polar Molecules on a Molecular Surface."

J. Phys. Chem. B **105**(1): 2881-2884.

Ishida, T., N. Choi, W. Mizutani, H. Tokumoto, I. Kojima, H. Azebara, H. Hokari, U. Akiba, and M. Fujihira (1999).

"High-Resolution X-ray Photoelectron Spectra of Organosulfur Monolayers on Au(111): S(2p) Spectral Dependence on Molecular Species."

Langmuir **15**(20): 6799-6806.

Jäger, B., H. Schürmann, H. U. Müller, H.-J. Himmel, M. Neumann, M. Grunze, and C. Wöll (1997).

Zeitschrift für Phys. Chem. **202**: 263.

Kakimura, K., and Y. Sakai (1979).

"The properties of GaAs-Al<sub>2</sub>O<sub>3</sub> and InP-Al<sub>2</sub>O<sub>3</sub> interfaces and the fabrication of MIS field-effect transistors."

Thin Solid Films **56**: 215-223.

Kang, J. F., R. Jordan, and A. Ulman (1998).

“Wetting and Fourier Transform Infrared Spectroscopy Studies of Mixed Self-Assembled Monolayers of 4'-Methyl-4-mercaptobiphenyl and 4'-Hydroxy-4-mercaptobiphenyl.”

Langmuir **14**: 3983-3985.

Kang, J. F., A. Ulman, R. Jordan, and D. G. Kurth (1999).

“Optically Induced Band Shifts in Infrared Spectra of Mixed Self-assembled Monolayers of Biphenyl Thiols.”

Langmuir **15**: 5555-5559.

Kang, J. F., A. Ulman, S. Liao, R. Jordan, G. Yang, and G.-y. Liu (2001).

“Self-Assembled Rigid Monolayers of 4'-Substituted-4-mercaptobiphenyls on Gold and Silver Surfaces.”

Langmuir **17**: 95-106.

Kitaigorodskii, I. A. (1961).

“Organic Chemical Crystallography”

New York, Consultants Bureau.

Laibinis, P. E., G. M. Whitesides, D. L. Allara, Y.-T. Tao, A. N. Parikh, and R. G. Nuzzo (1991).

“Comparison of the Structures and Wetting Properties of Self-Assembled Monolayers of n- Alkanethiols on the Coinage Metal Surfaces, Cu, Ag, Au'.”

J. Am. Chem. Soc. **113**: 7152-7167.

Leung, T. Y. B., P. Schwartz, G. Scoles, F. Schreiber, and A. Ulman (2000).

“Structure and growth of 4-methyl-4'-mercaptobiphenyl monolayers on Au(111): a surface diffraction study.”

Surf. Sci. **458**: 34-52.

Lide, D. R. (1997).

“Handbook of Chemistry and Physics”

New York, CRC Press Inc.

Lii, J.-H., and N. L. Allinger (1989).

“Molecular Mechanics. The MM3 Force Field for Hydrocarbons. 3. The van der Waals' Potentials and Crystal Data for Aliphatic and Aromatic Hydrocarbons.”

J. Am. Chem. Soc. **111**(23): 8576-8582.

Lindau, I., and W. E. Spicer (1974).

“The Probing Depth in Photoemission and Auger-Electron Spectroscopy.”

J. Electron Spectrosc. **3**: 409-413.

Luber, S. M., K. Adlkofer, U. Rant, A. Ulman, A. Götzhäuser, M. Grunze, D. Schuh, M. Tanaka, M. Tornow, and G. Abstreiter (in print).

“Liquid phase sensors based on chemically functionalized GaAs/AlGaAs heterostructures.”

Pysica E.

Luber, S. M., K. Adlkofer, U. Rant, A. Ulman, M. Grunze, D. Schuh, M. Tanaka, M. Tornow, and G. Abstreiter (2002).

“Chemically Passivated GaAs/AlGaAs Heterostructure HEMTs for Biosensor Applications.”

Proc. ICPS.

Lunt, S. R., G. N. Ryba, P. G. Santangelo, and N. S. Lewis (1991).

“Chemical studies of the passivation of GaAs surface recombination using sulfides and thiols.”

J. Appl. Phys. **70**(12): 7449-7467.

Macdonald, J. R., Ed. (1987).

"Impedance Spectroscopy"

New York, John Wiley & Sons.

Mao, D., A. Kahn, G. Le Lay, M. Marsi, Y. Hwu, G. Margaritondo, M. Santos, M. Shayegan, L. T. Florez, and J. P. Harbison (1991).

“Surface photovoltage and band bending at metal/GaAs interfaces: A contact potential difference and photoemission spectroscopy study.”

J. Vac. Sci. Technol. B **9**: 2083-2089.

Menezes, S., and B. Miller (1983).

“Surface and Redox Reactions at GaAs in Various Electrolytes.”

J. Electrochem. Soc. **130**(2): 517-523.

Miller, E. A., and G. L. Richmond (1997).

“Photocorrosion of n-GaAs and Passivation by Na<sub>2</sub>S: A comparison of the (100), (110), and (111)B Faces.”

J. Phys. Chem. B **101**: 2669-2677.

Moulder, J. F., W. E. Stickle, P. E. Sobol, and K. D. Bomben (1992).

"Handbook of X-ray Photoelectron Spectroscopy", Perkin-Elmer Corp.: Eden Prairie, MN.

Nakagawa, O. S., S. Ashok, C. W. Sheen, J. Märtensson, and D. L. Allara (1991).

“GaAs Interfaces with Octadecyl Thiol Self-Assembled Monolayer: Structural and Electrical Properties.”

Jap. J. Appl. Phys. **30**(12B): 3759-3762.

- Neuberger, R., G. Müller, O. Ambacher, and M. Stutzmann (2001).  
“High-electron-mobility AlGaIn/GaN transistors (HEMTs) for fluid monitoring applications.”  
*Physica Status Solidi A - Applied Research* **185**(1): 85-89.
- Nyburg, S. C., and H. Lüth (1972).  
“n-Octadecane: a correction and refinement of the structure given by Hayashida.”  
*Acta Crystallogr. B* **28**: 2992-2995.
- Owens, D. K., and R. C. Wendt (1969).  
“Estimation of the Surface Free Energy of Polymers.”  
*J. Appl. Polym. Sci.* **13**(3): 1741-1747.
- Palik, E. D., Ed. (1985).  
“Handbook of Optical Constants of Solids”  
Orlando, Academic Press, Inc.
- Powell, C. J. (1974).  
“Attenuation Length of Low-Energy Electrons in Solids.”  
*Surf. Sci.* **44**: 29-46.
- Rong, H.-T., S. Frey, Y.-J. Yang, M. Zharnikov, M. Buck, M. Whn, C. Wöll, and G. Helmchen (2001).  
“On the Importance of the Headgroup Substrate Bond in Thiol Monolayers: A Study of Biphenyl-Based Thiols on Gold and Silver.”  
*Langmuir* **17**(5): 1582-1593.
- Sabatani, E., J. Cohen-Boulakia, M. Bruening, and I. Rubinstein (1993).  
“Thioaromatic Monolayers on Gold: A New Family of Self-Assembling Monolayers.”  
*Langmuir* **9**: 2974-2981.
- Sackmann, E., and M. Tanaka (2000).  
“Supported membranes on soft polymer cushions: fabrication, characterization and applications.”  
*Trends Biotechnol.* **18**(2): 58-64.
- Schöning, M. J. (2001).  
“Novel Concepts for Silicon-Based Biosensors.”  
*Phys. Stat. Sol. a* **185**(1): 65-77.
- Seker, F., K. Meeker, T. F. Kuech, and A. B. Ellis (2000).  
“Surface Chemistry of Prototypical Bulk II-VI and III-V Semiconductors and Implications for Chemical Sensing.”  
*Chem. Rev.* **100**: 2505-2536.

Shaporenko, A., K. Adlkofer, L. S. O. Johansson, M. Tanaka, and M. Zharnikov (2003).

“Functionalization of GaAs Surfaces with Aromatic Self-Assembled Monolayers: A Synchrotron-Based Spectroscopic Study.”

Langmuir **19**: 4992-4998.

Sheen, C. W., J. X. Shi, J. Martenson, and D. L. Allara (1992).

“A New Class of Organized Self-Assembled Monolayers: Alkane Thiols on GaAs (100).”

J. Am. Chem. Soc. **114**: 1514-1515.

Shin, J., K. M. Geib, and C. W. Wilmsen (1991).

“Sulfur bond to GaAs.”

J. Vac. Sci. Technol. B **9**: 2337-2341.

Stocker, H. J., and D. E. Aspnes (1982).

“Surface chemical reactions on  $\text{In}_{0.53}\text{Ga}_{0.47}\text{As}$ .”

Appl. Phys. Lett. **42**(1): 85-87.

Stöhr, J. (1992).

“NEXAFS Spectroscopy”

Berlin, Springer-Verlag.

Stöhr, J., and D. A. Outka (1987).

“Determination of molecular orientations on surfaces from the angular dependence of near-edge x-ray-adsorption fine-structure spectra.”

Phys. Rev. B **36**(15): 7891-7905.

Takiguchi, H., K. Sato, T. Ishida, K. Abe, K. Yase, and K. Tamada (2000).

“Delicate Surface Reaction of Dialkyl Sulfide Self-Assembled Monolayers on Au(111).”

Langmuir **16**(4): 1703-1710.

Tao, Y.-T., C.-C. Wu, J.-Y. Eu, W.-L. Lin, K.-C. Wu, and C.-h. Chen (1997).

“Structure Evolution of Aromatic-Derivatized Thiol Monolayers on Evaporated Gold.”

Langmuir **13**: 4018-4023.

Taylor, D. M., and G. F. Bayes (1994).

“Calculating the surface potential of unionized monolayers.”

Phys. Rev. B **49**(2): 1439-1449.

Trotter, J. (1961).

“The crystal and molecular structure of biphenyl.”

Acta Crystallogr. **14**: 1135.

Tufts, B. J., L. G. Casagrande, N. S. Lewis, and F. J. Grunthar (1990).  
"Erratum: Correlations between the interfacial chemistry and current-voltage behavior of n-GaAs/liquid junctions."  
Appl. Phys. Lett. **57**(21): 2262-2264.

Uhlendorf, I., R. Reinecke-Koch, and R. Memming (1995).  
"Investigation of the Kinetics of Redox Reactions at GaAs Electrodes by Impedance Spectroscopy."  
J. Phys. Chem. **100**: 4930-4936.

Ulman, A. (1991).  
"An Introduction to Ultrathin Organic Films: From Langmuir-Blodgett to Self-Assembly"  
Boston, Academic Press.

Ulman, A. (1996).  
"Formation and Structure of Self-Assembled Monolayers."  
Chem. Rev. **96**: 1533-1554.

Ulman, A. (2001).  
"Self-Assembled Monolayers of 4-Mercaptobiphenyls."  
Acc. Chem. Res. **34**: 855-863.

Vager, Z., and R. Naaman (2002).  
"Surprising electronic-magnetic properties of close-packed organized organic layers."  
Chem. Phys. **281**(2-3): 305-309.

Vilan, A., J. Ghabboun, and D. Cahen (2003).  
"Molecule-Metal Polarization at Rectifying GaAs Interfaces."  
J. Phys. Chem. B **107**(26): 6360-6376.

Wagner, C. D., W. M. Riggs, L. E. Davis, and J. F. Moulder (1978).  
"Handbook of X-Ray Photoelectron Spectroscopy"  
Eden Prairie, Minnesota 55344, Perkin-Elmer Corporation, Physical Electronics Division.

Weast, R. C. (1970).  
"Handbook of Chemistry and Physics"  
Cleveland, The Chemical Rubber Co.

Weiss, K., S. Gebert, M. Wühn, H. Wadehol, and C. Wöll (1998).  
"Near edge x-ray absorption fine structure study of benzene adsorbed on metal surfaces: Comparison to benzene cluster complexes."  
J. Vac. Sci. Technol. A **16**(3): 1017-1022.

- Wirde, M., U. Gelius, T. Dunbar, and D. L. Allara (1997).  
“Modification of self-assembled monolayers of alkanethiols on gold by ionizing radiation.”  
Nuc. Instrum. Meth. Phys. Res. B **131**: 245-251.
- Wu, G. W., D. Cahen, P. Graf, R. Naaman, A. Nitzan, and D. Shvarts (2001).  
“Direct Detection of Low-Concentration NO in Physiological Solutions by a New GaAs-Based Sensor.”  
Chem. Eur. J. **7**(8): 1743-1749.
- Yang, Y. W., and L. J. Fan (2002).  
“High-Resolution XPS Study of Decanethiol on Au(111): Single Sulfur-Gold Bonding Interaction.”  
Langmuir **18**(4): 1157-1164.
- Yeh, J. J., and I. Lindau (1985).  
At. Data Nucl. Data Tables **32**: 1.
- Yokoyama, T., K. Seki, I. Morisada, K. Edamatsu, and T. Ohta (1990).  
Phys. Scr. **41**: 189.
- Zharnikov, M., S. Frey, K. Heister, and M. Grunze (2000).  
“Modification of Alkanethiolate Monolayers by Low Energy Electron Irradiation: Dependence on the Substrate Material and on the Length and Isotopic Composition of the Alkyl Chains.”  
Langmuir **16**(6): 2697-2705.
- Zharnikov, M., and M. Grunze (2001).  
“Spectroscopic characterization of thiol-derived self-assembling monolayers.”  
J. Phys.: Condens. Matter. **13**: 11333–11365.
- Zharnikov, M., and M. Grunze (2002).  
“Modification of thiol-derived self-assembling monolayers by electron and x-ray irradiation: Scientific and lithographic aspects.”  
J. Vac. Sci. Technol. B **20**(5): 1793-1807.
- Zharnikov, M., A. Küller, A. Shaporenko, E. Schmidt, and W. Eck (2003).  
“Aromatic Self-Assembled Monolayers on Hydrogenated Silicon.”  
Langmuir **19**(11): 4682-4687.



## Publications

### ***Published Manuscripts Relevant to this Study***

Adlkofer, K., W. Eck, M. Grunze, and M. Tanaka (2003).

“Surface Engineering of Gallium Arsenide with 4-Mercaptobiphenyl Monolayers.”  
J. Phys. Chem. B **107**(2): 587-591.

Adlkofer, K., A. Shaporenko, M. Zharnikov, M. Grunze, A. Ulman, and M. Tanaka (2003).

“Chemical Engineering of Gallium Arsenide Surfaces with 4'-Methyl-4-Mercaptobiphenyl and 4'-Hydroxy-4-Mercaptobiphenyl Monolayers.”  
J. Phys. Chem B. **107**(42): 11737-11741.

Shaporenko, A., K. Adlkofer, L. S. O. Johansson, M. Tanaka, and M. Zharnikov (2003).

“Functionalization of GaAs Surfaces with Aromatic Self-Assembled Monolayers: A Synchrotron-Based Spectroscopic Study.”  
Langmuir **19**: 4992-4998.

Luber, S. M., K. Adlkofer, U. Rant, A. Ulman, A. Götzhäuser, M. Grunze, D. Schuh, M. Tanaka, M. Tornow, and G. Abstreiter (in print)

“Liquid phase sensors based on chemically functionalized GaAs/AlGaAs heterostructures.”  
Pysica E in print.

Luber, S. M., K. Adlkofer, U. Rant, A. Ulman, M. Grunze, D. Schuh, M. Tanaka, M. Tornow, and G. Abstreiter (2002).

“Chemically Passivated GaAs/AlGaAs Heterostructure HEMTs for Biosensor Applications.”  
Proc. ICPS.

### ***Other Published Manuscripts***

Adlkofer, K., M. Tanaka, H. Hillebrandt, G. Wiegand, E. Sackmann, T. Bolom, R. Deutschmann, and G. Abstreiter (2000).

“Electrochemical passivation of gallium arsenide surface with organic self-assembled monolayers in aqueous electrolytes.”  
Appl. Phys. Lett. **76**(22): 3313-3315.

Adlkofer, K., and M. Tanaka (2001).

“Stable Surface Coating of Gallium Arsenide with Octadecylthiol Monolayers.”  
Langmuir **17**(14): 4267-4273.

Adlkofer, K., E. F. Duijs, F. Findeis, M. Bichler, A. Zrenner, E. Sackmann, G. Abstreiter, and M. Tanaka (2002).

“Enhancement of photoluminescence from near-surface quantum dots by suppression of surface state density.”

Phys. Chem. Chem. Phys. **4**: 785-790.

Duijs, E. F., F. Findeis, R. A. Deutschmann, M. Bichler, A. Zrenner, G. Abstreiter, K. Adlkofer, M. Tanaka, and E. Sackmann (2001).

“Influence of Thiol Coupling on Photoluminescence of Near Surface InAs Quantum Dots.”

Phys. Status Solidi B **3**: 871-875.

Purrucker, O., H. Hillebrandt, K. Adlkofer, and M. Tanaka (2001).

“Deposition of highly resistive lipid bilayer on silicon–silicon dioxide electrode and incorporation of gramicidin studied by ac impedance spectroscopy.”

Electrochem. Acta **47**: 791-798.

Tutus, M., O. Purrucker, K. Adlkofer, M. Eickhoff, and M. Tanaka (submitted)

„Electrochemical Stabilization of Crystalline Silicon with Aromatic Self-Assembled Monolayers in Aqueous Electrolytes.”

J. Appl. Phys. submitted.

## ***Comments and Published Abstracts***

Adlkofer, K., M. Tanaka, E. Sackmann, E. F. Duijs, F. Findeis, A. Zrenner, M. Bichler, and G. Abstreiter (2000)

“Enhancement of Photoluminescence Properties of Quantum Dots by Thin Organic Films.”

Eur. Biophys. J. **29**: 375

Adlkofer, K., E. Sackmann, and M. Tanaka (2002).

“Comment on “Structural characterization of GaAs/thiol/electrolyte interface”

[Mater. Lett. **46** (2000) 320–326].”

Mat. Lett. **54**: 89-91.

## Lebenslauf

**Name:** Klaus Adlkofer  
**Geburtsdatum:** 12. Oktober 1972  
**Nationalität:** deutsch

### ***Ausbildung:***

#### Promotion:

08/2000 – 12/2003      Promotion in Physik an der Technischen Universität München, Lehrstuhl für Biophysik (Prof. E. Sackmann), Thema: Engineering of Bulk and Nanostructured GaAs with Organic Monomolecular Films

#### Studium:

22.05.2000      Diplom in Physik, Technische Universität München

05/1999 – 05/2000      Diplomarbeit an der Technischen Universität München, Lehrstuhl für Biophysik (Prof. E. Sackmann), Thema: Functionalization of GaAs Surfaces with Organic Molecular Assemblies

1993 – 2000      Studium der Allgemeinen Physik an der Technischen Universität München

#### Schule:

1992      Abitur  
1983 – 1992      Christoph-Scheiner-Gymnasium Ingolstadt  
1981 – 1983      Grundschule Walting  
1979 – 1981      Grundschule Arnsberg

### ***Zivildienst:***

1992 – 1993      Fahrdienst und Überwachung, Malteser Hilfsdienst, Ingolstadt